

A Data-Driven Evolutionary Transfer Optimization for Expensive Problems in Dynamic Environments *

Ke Li¹, Renzhi Chen² and Xin Yao²

¹Department of Computer Science, University of Exeter, EX4 4QF, Exeter, UK

²National Innovation Institute of Defence Technology, Beijing, China

³Department of Computer Science and Engineering, Southern University of Science and Technology, Shenzhen 518055, China

*Email: k.li@exeter.ac.uk

Abstract: Many real-world problems are usually computationally costly and the objective functions evolve over time. Data-driven, a.k.a. surrogate-assisted, evolutionary optimization has been recognized as an effective approach for tackling expensive black-box optimization problems in a static environment whereas it has rarely been studied under dynamic environments. This paper proposes a simple but effective transfer learning framework to empower data-driven evolutionary optimization to solve dynamic optimization problems. Specifically, it applies a hierarchical multi-output Gaussian process to capture the correlation between data collected from different time steps with a linearly increased number of hyperparameters. Furthermore, an adaptive source task selection along with a bespoke warm starting initialization mechanisms are proposed to better leverage the knowledge extracted from previous optimization exercises. By doing so, the data-driven evolutionary optimization can jump start the optimization in the new environment with a strictly limited computational budget. Experiments on synthetic benchmark test problems and a real-world case study demonstrate the effectiveness of our proposed algorithm against nine state-of-the-art peer algorithms.

Keywords: Multi-output Gaussian processes, kernel methods, dynamic optimization, transfer optimization, data-driven evolutionary optimization.

1 Introduction

Real-world black-box optimization problems are complex and challenging not only because they are non-convex, multi-modal, highly constrained, multi-objective, but also subject to various uncertainties. In particular, dynamic optimization problem (DOP), where the objective function(s) experience abrupt changes over time with temporally changing/evolving optima, is ubiquitous in many real-world optimization scenarios. For example, modern software systems are usually configurable with a set of known control features (e.g., CPU cap, thread pool size and cache size) that affect the system's functional and non-functional properties. To adapt to the requirements of many end-users concurrently, those control features need to be configured dynamically on-the-fly according to the changing runtime environments, e.g., bandwidth and response time [1].

Partially due to the population-based property and the self-adaptivity [2], evolutionary algorithms (EAs) have been widely recognized as an effective tool for DOPs. Most EA developments implicitly assume that the objective function evaluations (FEs) are computationally cheap or trivial. Thus, it is common to see an EA routine costs at least tens or hundreds thousands or even more FEs in a single run. Unfortunately, such assumption usually does not stand in real-world optimization scenarios where FEs are physically, computationally or economically expensive, as known as expensive black-box optimization. It becomes more challenging when the environments dynamically change with time and are full of uncertainties.

The Gaussian process (GP) model [3], also known as Kriging [4] or design and analysis of computer experiments (DACE) stochastic process model [5], has been widely recognized as one of the most ef-

*This manuscript is submitted for potential publication. Reviewers can use this version in peer review.

efficient and effective tools for dealing with expensive black-box optimization problems [6–8]. Its basic assumption is built upon a GP from which each testing point is sampled. The distribution of any unknown point is estimated based on the data collected from the previous search. The update of the GP model is guided by the optimization of an acquisition function, e.g., expected improvement [6], probability of improvement [7] and upper confidence bound [9], that implements a principled exploitation versus exploration balance over the surrogate landscape. In practice, the GP model constitutes the foundation of data-driven optimization approaches, including but not limited to the efficient global optimization (EGO) [10] and the Bayesian optimization (BO) [8], for expensive black-box optimization problems. There also have been many efforts devoted to the use of GP and other machine learning models under the banner of EAs, as known as surrogate-assisted EAs (SAEAs) [11, 12]. Surprisingly, the existing data-driven optimization endeavors have been extensively dedicated for the continuous space with static objective function(s), whereas few works (only [13–16] to the best of our knowledge) have been done for DOPs. This can be attributed to the following two imperative challenges.

- The ultimate goal of dynamic optimization is no longer merely approximating the global optimum, but to track the evolving optimum over time. Due to the dynamic environments and the fast moving problem landscapes, it is almost impossible or at least ineffective and inefficient to restart, also known as ‘cold start’, the optimization routine from scratch when the environment changes, e.g., the first four strategies proposed in [13].
- Although most data-driven optimization approaches have the ability to adapt to the underlying search landscapes, it is not wise to simply ignore the changes but just let the optimization routine run. The time-varying nature of the DOP itself renders the data collected in previous time steps become less reliable or even harmful for model building in the current time step, e.g., [13–15, 17]. Furthermore, excessive data turn the training and inference of a GP model into a computationally expensive practice.

Note that DOPs implicitly assume certain correlations between problem landscapes of recent time steps, given that many applications usually experience a gentle change from one stage to the next. Therefore, it is reasonable to selectively leverage the data collected from the previous search processes to ‘warm start’ the underlying optimization task. In fact, warm starting a BO has been studied in the machine learning community such as hyperparameter optimization [18] and neural architecture search [19]. However, they are mainly a ‘one-off’ process that aims to transfer knowledge/experience learned from the existing data to ‘jump start’ the underlying problem-solving process. This is in principle a static version of our dynamic optimization scenario from one time step to the next in particular whereas the problem-solving tasks and problem landscapes continuously change over time.

Very recently, we have developed a simple BO variant [17], dubbed **TBO**, that uses a multi-output GP (MOGP) [20] to exploit and leverage the correlations between different time steps, instead of modeling each of which individually. The proof-of-concept results have demonstrated the effectiveness of **TBO** for solving DOPs in comparison to some peer algorithms with a limited computational budget. However, it is far from mature in view of the following three drawbacks.

- The number of hyperparameters of the conventional MOGP is cubic of the number of tasks. In our dynamic optimization scenario, it is highly unlikely to collect abundant data at each time step since each FE is costly. In this case, the increase of data can hardly match the overflow of the number of hyperparameters. This can make the MOGP to be underfit with the time step goes by.
- In **TBO**, it applies a simple decay mechanism to proactively dump some previously collected data in case they are less relevant to the current time step, to mitigate the notoriously time-consuming of MOGP. However, since this decay mechanism is augmented as a hyperparameter of MOGP, it not only aggravates the risk of overfitting given the limited training data in expensive optimization, but also does not provide a controllable method to pick up the most relevant source for the MOGP model training.
- Last but not the least, one of the advantages of **TBO** is that it only needs to sample a limited number of initial solutions to jump start the new optimization task by MOGP. However, since

this sampling at the initialization step is conducted in a random manner, it can easily be biased and the knowledge about the previous optimization tasks cannot be fully exploited.

Bearing these concerns in mind, this paper proposes a principled data-driven transfer optimization framework, dubbed DETO, for expensive DOPs. The main contributions of this paper are outlined as follows.

- To mitigate the underfitting problem of the conventional MOGP, we propose a hierarchical MOGP that replaces the block matrices of the task related hyperparameters of the MOGP with a series of masked block matrices.
- To mitigate the risk of overfitting caused by the augmented hyperparameter(s), we develop an adaptive source data selection mechanism to proactively pick up the most suitable source task for MOGP model training.
- To enforce a strategic jump start at the outset of a new optimization task, we propose a bespoke initialization strategy by leveraging the local optima collected from the estimated problem landscapes of the previously finished optimization tasks, each of which is represented as a GP models respectively.
- To overcome the non-convex property of optimizing the acquisition function, we propose a simple but effective EA with local search to search for the next point of merit.
- Extensive experiments on both synthetic benchmark problems with controllable dynamic characteristics and a real-world dynamic optimization problem fully demonstrate the effectiveness our proposed DETO in comparison to other nine peer algorithms.

The rest of this paper is organized as follows. Section 2 provides some important background knowledge in order to understand this paper along with a pragmatic literature review. The technical details of our proposed DETO are delineated in Section 3 and its performance is validated through a series of empirical studies given in Section 5. At the end, Section 6 concludes this paper and shed some lights on future directions.

2 Preliminaries

This section starts with some preliminary knowledge including the formal definition of DOP considered in this paper and the basic idea of a vanilla data-driven optimization method based on the GP model. Then, we give a pragmatic literature review on both data-driven methods (EGO and BO variants in particular) and EAs for solving DOPs.

2.1 Problem Definition

The DOP considered in this paper is defined as:

$$\begin{aligned} & \text{maximize } f(\mathbf{x}, t) \\ & \text{subject to } \mathbf{x} \in \Omega \end{aligned} \quad (1)$$

where $\mathbf{x} = (x_1, \dots, x_n)^\top$ is a decision vector (variable), $\Omega = [x_i^L, x_i^U]_{i=1}^n \subset \mathbb{R}^n$ is the search space, $t \in \{1, \dots, T\}$ is a discrete time step and $T > 1$ is the total number of time steps. Note that the objective function is assumed to be *computationally expensive* and it changes over time so as its landscapes and the local/global optima. In this case, the ultimate goal of computationally expensive black-box optimization in dynamic environments is to track the time-varying optimum across T time steps under a strictly limited amount of overall computational budget.

Algorithm 1: Pseudo code for a vanilla data-driven optimization based on GP model

Input: Related hyperparameter settings.

Output: The best solution found so far.

- 1 Use an experimental design method to sample a set of initial solutions $\mathcal{X} \leftarrow \{\mathbf{x}^i\}_{i=1}^{N_I}$ from Ω and evaluate their objective function values $\mathcal{Y} \leftarrow \{f(\mathbf{x}^i)\}_{i=1}^{N_I}$. Set the initial training dataset $\mathcal{D} \leftarrow \{(\mathbf{x}^i, f(\mathbf{x}^i))\}_{i=1}^{N_I}$;
 - 2 **while** *termination criteria is not met* **do**
 - 3 Build a GP model based on \mathcal{D} ;
 - 4 Optimize an acquisition function to obtain a candidate solution $\hat{\mathbf{x}}^*$;
 - 5 Evaluate the objective function values of $\hat{\mathbf{x}}^*$ and update $\mathcal{D} \leftarrow \mathcal{D} \cup \{(\hat{\mathbf{x}}^*, f(\hat{\mathbf{x}}^*))\}$;
 - 6 **return** $\operatorname{argmin}_{\mathbf{x} \in \mathcal{D}} f(\mathbf{x})$
-

Theorem 1. (*Karush-Kuhn-Tucker conditions [21]*) If \mathbf{x}^* is a local optimum of an objective function $f(\mathbf{x}) : \mathbb{R}^n \rightarrow \mathbb{R}$ with m constraints $\{g_i(\mathbf{x}) \leq 0\}_{i=1}^m$ and the set of vectors $\{\nabla g_j(\mathbf{x}^*) | j \text{ is the index of an active constraint}\}$ are linearly independent. There exists a vector $\mu = (\mu_1, \dots, \mu_m)^\top \in \mathbb{R}^m$, such that:

$$\begin{aligned} \nabla f(\mathbf{x}^*) + \sum_{j=1}^m \mu_j \nabla g_j(\mathbf{x}^*) &= 0, \\ \mu_j g_j(\mathbf{x}^*) |_{j=1}^m &= 0 \end{aligned} \tag{2}$$

where $\mu_i \geq 0, \forall i \in \{1, \dots, m\}$.

Remark 1. The objective and constraint functions are assumed to be continuously differentiable in the Karush-Kuhn-Tucker (KKT) conditions.

Remark 2. The objective function considered in this paper does not include constraints, thus we ignore the $\sum_{j=1}^m \mu_j \nabla g_j(\mathbf{x}^*)$ part of equation (2) in the latter derivations.

2.2 Vanilla Data-Driven Optimization Based on GP Model

Data-driven optimization based on GP model is a class of sequential model-based optimization methods for solving black-box optimization problems with computationally expensive objective function(s). As shown in the line 1 of Algorithm 1, it starts from uniformly sampled solutions according to a space-filling experimental design (e.g., Latin hypercube sampling). Thereafter, it sequentially updates its next sample until the computational budget is exhausted.

The data-driven optimization based on GP model consists of two main components: *i*) a surrogate model based on GP for approximating the expensive objective function; and *ii*) an infill criterion (based on the optimization of an acquisition function) that decides the next sampling point for being evaluated by the actual expensive objective function. We briefly introduce these two components as follows.

2.2.1 Surrogate Model

This paper considers using GP regression (GPR) model to serve the surrogate modeling (line 3 of Algorithm 1). Given a set of training data $\mathcal{D} = \{(\mathbf{x}^i, f(\mathbf{x}^i))\}_{i=1}^N$, the GPR model considered in this paper aims to learn a noise-free latent function with a constant 0 mean. For each testing input vector $\mathbf{z}^* \in \Omega$, the mean and variance of the target $f(\mathbf{z}^*)$ are predicted as:

$$\begin{aligned} \mu(\mathbf{z}^*) &= \mathbf{k}^{*T} K^{-1} \mathbf{f} \\ \sigma(\mathbf{z}^*) &= k(\mathbf{z}^*, \mathbf{z}^*) - \mathbf{k}^{*T} K^{-1} \mathbf{k}^* \end{aligned} \tag{3}$$

where $X = (\mathbf{x}^1, \dots, \mathbf{x}^N)^\top$ and $\mathbf{f} = (f(\mathbf{x}^1), \dots, f(\mathbf{x}^N))^\top$. $\mathbf{m}(X)$ is the mean vector of X , \mathbf{k}^* is the covariance vector between X and \mathbf{z}^* , and K is the covariance matrix of X . In particular, a covariance

function, also known as a kernel function, is used to measure the *similarity* between a pair of two data points \mathbf{x} and $\mathbf{x}' \in \Omega$. Here we use the radial basis function (RBF) kernel in this paper and it is defined as:

$$k(\mathbf{x}, \mathbf{x}') = \gamma \exp\left(-\frac{\|\mathbf{x} - \mathbf{x}'\|}{\ell}\right)^2, \quad (4)$$

with two hyperparameters γ and length scale ℓ . The predicted mean $\mu(\mathbf{z}^*)$ is directly used as the prediction of $f(\mathbf{z}^*)$, and the predicted variance $\sigma(\mathbf{z}^*)$ quantifies the uncertainty. As recommended in [3], the hyperparameters associated with the mean and covariance functions are learned by maximizing the log marginal likelihood function defined as:

$$\log p(\mathbf{f}|X) = -\frac{1}{2}\mathbf{f}^\top K^{-1}\mathbf{f} - \frac{1}{2}\log |K| - \frac{N}{2}\log 2\pi. \quad (5)$$

2.2.2 Infill Criterion

Instead of optimizing the surrogate objective function, the search for the next point of merit $\hat{\mathbf{x}}^*$ is driven by an acquisition function that strikes a balance between exploitation of the predicted minimum and exploration of model uncertainty:

$$\hat{\mathbf{x}}^* = \operatorname{argmax}_{\mathbf{x} \in \Omega} f^{\text{acq}}(\mathbf{x}), \quad (6)$$

where $f^{\text{acq}}(\mathbf{x}) = \mu(\mathbf{x}) + \omega\sigma(\mathbf{x})$ is the widely used upper confidence bound (UCB) [6] in this paper. In particular, $\omega > 0$ is a parameter that controls the trade-off between exploration and exploitation. The optimization of (6) can be carried out by either an EA or a gradient descent method (lines 4 and 5 of Algorithm 1).

2.3 Related Works

This subsection gives a pragmatic overview of related works for handling DOPs from the data-driven and evolutionary optimization perspectives respectively.

2.3.1 Data-Driven Optimization

As briefly introduced in Section I, there is few prior works on expensive dynamic optimization from the data-driven optimization perspective. To the best of our knowledge, Kushner [22] is the first who proposed to model a dynamically changing function by using a stochastic processes model. However, only one dimensional problem was considered in [22] which is far from useful in practical scenarios. Afterwards, this topic has been kept silent and lied down for years until Morales-Enciso and Branke proposed eight strategies to handle expensive DOPs under the EGO framework [13]. In particular, the first four simple and straightforward strategies including random sampling, evolutionary mutation, restart and ignorance; while the latter four are proposed to reuse and transfer previous knowledge to the underlying problem-solving process. Obviously, these are too simple to be effective for handling complex dynamics. Although the other four strategies proposed in [13] aim to selectively leverage the previous information by augmenting the covariance function in GP model building, they are subject to some prior knowledge/assumption of the characteristics of the underlying problem. Recently, Nyikosa et al. [14] proposed an adaptive BO that uses a product kernel to augment a spatial-temporal covariance function for handling expensive DOPs. The temporal part is used as a forgetting factor that helps adaptively choose different old data in the GP model training and inference. This is implemented by a time-related length-scale parameter that can be learned as an additional hyperparameter in a maximum likelihood estimation. In [15], two approaches were proposed to enable BO for solving DOPs. One is called window approach that only uses the most recent observations for GP model training; and the other is called time-as-covariate approach that augments the time into the covariance function. Very recently, we proposed a BO variant [17] that provides a proof-of-concept result of using a MOGP to leverage the correlation between the current optimization task with the previous ones. To mitigate the soaring computational cost, a simple sliding window strategy is applied to merely focus on the most recent time steps.

Another related line of research is ‘warm starting’ a data-driven optimization by using additional information besides the FEs. Especially in the BO community, a large body of literature promotes the idea to meta-learn models [23, 24] or acquisition function [25, 26], to transfer knowledge by weighted aggregating surrogate models across various tasks [18, 27, 28], and to conduct multi-tasking [29]. These methods have shown to be powerful for hyper-parameter optimization, but they usually require large amounts of historical training data to extract the characteristics of a class of tasks, which might hardly be met in the expensive dynamic optimization scenario considered in this paper.

2.3.2 Evolutionary Optimization

Due to the population-based and adaptive characteristics, EAs have been widely recognized as a powerful tool for DOPs. However, since EAs usually require tons of FEs to obtain a reasonable solution, it is not directly applicable and computationally unaffordable for expensive DOPs. In recent decades, there have been many efforts devoted to using EAs for solving DOPs, here we just give a pragmatic overview of some selected works according to the ways of handling dynamics. Interested readers are recommended to some excellent survey papers for a more comprehensive literature review, e.g., [30–34].

- *Diversity enhancement*: As its name suggests, the basic idea is to propel an already converged population jump out of the approximated optimum in the previous time step by increasing the population diversity. This is usually implemented by either responding to the dynamics merely after detecting a change of the environment or maintaining the population diversity throughout the whole optimization process. The prior one is known as diversity introduction and is usually accompanied by a change detection technique. For example, [35–37] developed some hypermutation methods by which the solutions are expected to jump out of their current positions and thus to adapt to the changed environment. In [38–40], some additional solutions, either generated in a random manner or by some heuristics, are injected into the current population to participate the survival competition. On the other hand, the latter one, called diversity maintenance, usually does not explicitly respond to the changing environment [41–43] whereas it mainly relies on its intrinsic diversity maintenance strategy to adapt to the dynamics. In addition to diversity introduction and maintenance, a multi-population approach is another alternative to handle dynamics by enhancing diversity. In particular, it mainly maintains multiple subpopulations concurrently, each of which is either responsible for a particular area in the search space [44, 45] or assigned with a specific task such as searching for the global optimum or tracking the dynamic environments [46–48].
- *Memory mechanism*: The major purpose of this type of method is to utilize the historical information to accelerate the convergence progress. In particular, the memory mechanism implicitly assumes that the DOPs are periodical or recurrent. In other words, the optima may return to the regions near their previous locations. In [49], researchers used redundant coding via diploid genomes as the implicit memory to encode history into the solution representation. In contrast, memory can also be maintained explicitly. For example, [50–52] directly stored the previous promising solutions or local optima visited in the previous time steps to inform the current search process. [53] exploited the historical knowledge and used it to build up an evolutionary environment model. Accordingly, this model is used to guide the adaptation to the changing environment.
- *Prediction strategy*: Since it is reasonable to anticipate some patterns associated with the changes in dynamic environments, the prediction strategy is usually coupled with a memory mechanism to reinitialize the population according to the learned patterns extracted from previous search experience. For example, [54] employed an autoregressive model, built upon the historical information, to seed a new population within the neighborhood of the anticipated position of the new optimal solution. By utilizing the regularity property of the Pareto set of continuous multi-objective optimization problems, [55] and [56] developed various models to capture the movement of the Pareto set manifolds’ centers under different dynamic environments. Instead

Algorithm 2: Pseudo code of DETO

Input: Related hyperparameter settings.

Output: The optima found at all time steps \mathcal{X}^* .

```
1  $t \leftarrow 1, \mathcal{D} \leftarrow \emptyset, \mathcal{X}^* \leftarrow \emptyset;$ 
2 Use an experimental design method to sample a set of initial solutions  $\mathcal{X}^1 \leftarrow \{(\mathbf{x}^i, t)\}_{i=1}^{N_I}$  from
    $\Omega$  and evaluate their objective function values  $\mathcal{Y} \leftarrow \{f((\mathbf{x}^i, t), t)\}_{i=1}^{N_I}$ . Set the initial training
   dataset  $\mathcal{D}^t \leftarrow \{((\mathbf{x}^i, t), f((\mathbf{x}^i, t), t))\}_{i=1}^{N_I}, N_t \leftarrow N_I;$ 
3 while  $t \leq T$  do
4   while  $N_t < N_t^{\text{FE}}$  do
6     Build a MOGP model based on  $\mathcal{A} \cup \mathcal{D}^t$  with a low-rank approximation of covariance
       matrix;
57    Optimize an acquisition function to obtain a candidate solution  $(\hat{\mathbf{x}}, t);$ 
8     Evaluate the objective function values of  $(\hat{\mathbf{x}}, t)$  and set
        $\mathcal{D}^t \leftarrow \mathcal{D}^t \cup \{((\hat{\mathbf{x}}, t), f((\hat{\mathbf{x}}, t), t))\};$ 
9      $N_t \leftarrow N_t + 1;$ 
10     $\mathcal{D} \leftarrow \mathcal{D} \cup \mathcal{D}^t;$ 
11     $\mathcal{X}^* \leftarrow \mathcal{X}^* \cup \left\{ \underset{(\mathbf{x}, t) \in \mathcal{D}^t}{\text{argmin}} f((\mathbf{x}, t), t) \right\};$ 
13     $t \leftarrow t + 1;$ 
14    Use the adaptive source data selection to pick up  $k$  related datasets from  $\mathcal{D};$ 
15    Use the warm starting initialization to generate  $k$  augmented datasets to construct  $\mathcal{A};$ 
16     $N_t \leftarrow 0, \mathcal{D}^t \leftarrow \emptyset;$ 
17 return  $\mathcal{X}^*$ 
```

of anticipating the position of the new optima when the environment changes, [57] suggested to predict the optimal moving direction of the population. More recently, [58] and [59] proposed a hybrid scheme, which uses the Kalman Filter or random re-initialization, alternatively, according to their online performance, to respond to the changing environment.

3 Proposed Algorithm

The pseudo code of DETO is given in Algorithm 2 which shares almost the same logic as the vanilla data-driven optimization based on GP model shown in Algorithm 1. The main differences (highlighted in light gray background) are: *i*) a hierarchical MOGP with a reduced number of hyperparameters as the surrogate model to leverage the information collected from the previous time steps; *ii*) an adaptive source data selection mechanism to mitigate the risk of overfitting; *iii*) a bespoke initialization mechanism that warm starts the new optimization task; and *iv*) a simple but effective EA variant with local search to search for the next point of merit.

3.1 Surrogate Model Building

Given a DOP, we denote $\mathcal{D} = \{\mathcal{D}^1, \dots, \mathcal{D}^T\}$ as a set of observations collected so far where $\mathcal{D}^t = \{((\mathbf{x}^k, t), f((\mathbf{x}^k, t), t))\}_{k=1}^{N_t}, t \in \{1, \dots, T\}, T \geq 1$ and $N_t > 1$ is the number of observations evaluated at the t -th time step. This paper proposes to apply a MOGP model to exploit the correlations between the observations collected at different time steps. Comparing to the conventional GPR model, the MOGP model is featured with the multi-output covariance function, also known as linear model of coregionalization (LMC) [20], defined as:

$$k((\mathbf{x}, t), (\mathbf{x}', t')) = \sum_{i=1}^T [A_i]_{t,t'} k_i(\mathbf{x}, \mathbf{x}'), \quad (7)$$

where (\mathbf{x}, t) is a candidate solution sampled at the current time step t while (\mathbf{x}', t') is an observation at the t' -th time step ($1 \leq t' \leq T$) chosen from \mathcal{D} . $k_i(*, *)$ is the covariance function at the i -th time step ($1 \leq i \leq T$) as in the conventional GPR. $A_i = B_i B_i^\top \in \mathbb{R}^{T \times T}$ is used to characterize the correlation between different time steps where

$$B_i = \begin{bmatrix} b_{1,1} & b_{1,2} & \cdots & b_{1,r} \\ b_{2,1} & b_{2,2} & \cdots & b_{2,r} \\ \vdots & \vdots & \ddots & \vdots \\ b_{T,1} & b_{T,2} & \cdots & b_{T,r} \end{bmatrix}, \quad (8)$$

where $b_{j,k}$ ($1 \leq j \leq T$ and $1 \leq k \leq r$) is the coefficient (as the hyperparameter) that aggregates the covariance between outputs across different time steps. For each testing input vector sampled at the t -th time step (\mathbf{z}^*, t) , the mean and variance of the target $f((\mathbf{z}^*, t), t)$ are predicted as:

$$\begin{aligned} \mu((\mathbf{z}^*, t)) &= \mathbf{k}_T^* K_T^{-1} \mathbf{f}_T \\ \sigma((\mathbf{z}^*, t)) &= k((\mathbf{z}^*, t), (\mathbf{z}^*, t)) - \mathbf{k}_T^* K_T^{-1} \mathbf{k}_T^* \end{aligned} \quad (9)$$

where \mathbf{f}_T is a vector of the objective values of all solutions in \mathcal{D} , \mathbf{k}_T^* is the covariance vector between (\mathbf{z}^*, t) and solutions in \mathcal{D} , and K_T is the covariance matrix of solutions in \mathcal{D} .

According to the equations (7) and (8), we can infer that the number of hyperparameters of the LMC is $\mathcal{O}(T^3)$, which grows cubically with the number of time steps. Given that the FEs considered in this paper are computationally expensive, we do not expect to collect abundant data across different time steps. In this case, we have the risk of underfitting the LMC in our expensive dynamic optimization scenario. To mitigate this issue, inspired by the hierarchical GP developed in [60], we propose a hierarchical MOGP (HMOGP) which keeps the covariance function the same as equation (7) but the task correlation matrix A_i is defined as:

$$A_i = \begin{cases} 1 & \text{if } t \geq i, t' \geq i \\ 0 & \text{otherwise} \end{cases}. \quad (10)$$

Alternatively, we can write A_i as:

$$A_i = \begin{bmatrix} \mathbf{0}_{(i-1) \times (i-1)} & \mathbf{1}_{(i-1) \times (T-i+1)} \\ \mathbf{1}_{(T-i+1) \times (i-1)} & \mathbf{1}_{(T-i+1) \times (T-i+1)} \end{bmatrix}. \quad (11)$$

More specifically, we have:

$$\begin{aligned} A_1 &= \begin{bmatrix} 1 & \cdots & 1 \\ \vdots & \ddots & \vdots \\ 1 & \cdots & 1 \end{bmatrix}, A_2 = \begin{bmatrix} 0 & 1 & \cdots & 1 \\ 1 & 1 & \cdots & 1 \\ \vdots & \vdots & \ddots & \vdots \\ 1 & 1 & \cdots & 1 \end{bmatrix}, \\ \cdots, A_T &= \begin{bmatrix} 0 & \cdots & 0 & 1 \\ \vdots & \ddots & \vdots & \vdots \\ 0 & \cdots & 0 & 1 \\ 1 & \cdots & 1 & 1 \end{bmatrix}. \end{aligned} \quad (12)$$

By doing so, the number of hyperparameters of this HMOGP is significantly reduced to two magnitudes of order as $\mathcal{O}(T)$, comparing against the conventional LMC.

3.2 Adaptive Source Data Selection Mechanism

During the process of dynamic optimization, we can expect the evaluated solutions are progressively accumulated with time. However, although it sounds to be counter-intuitive at first glance since the data collected during the expensive optimization is usually too limited to train an adequate model, accumulating an ‘excessive’ amount of data can lead to the risk of overfitting. In Fig. 1, we use

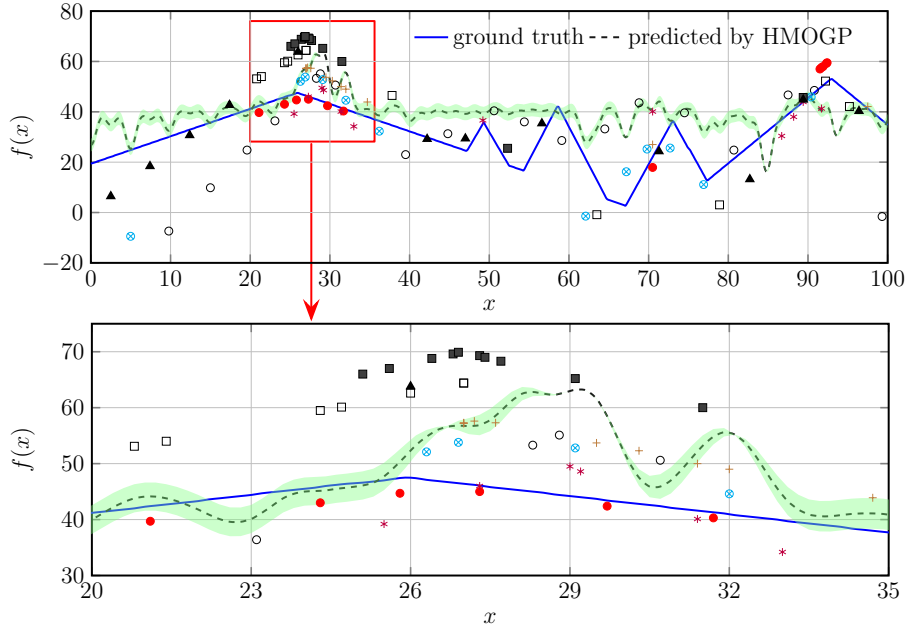


Figure 1: An illustrative example of an overfitting problem in HMOGP. Here we consider source tasks collected from the moving peak benchmark problem at 8 different time steps, which are represented as different marks.

the moving peak function considered in our empirical study in Section 4 to constitute an illustrative example. More specifically, we consider $T = 8$ time steps, each of which consists of 19 data points sampled from a uniform distribution within the range of \mathbf{x} of the moving peak function. As the example shown in Fig. 1, it is clear to see that the HMOGP becomes overfit with many unnecessary local optima by considering all data collected from 8 different source datasets. To mitigate this issue, we propose an adaptive source data selection mechanism to proactively pick up the most suitable previously collected source data to build the HMOGP at each time step. It contains four steps.

Step 1: Build a GPR model $\mathcal{GP}(\mathcal{D}^t)$, $t \in \{1, \dots, T-1\}$, for each of the previous time steps.

Step 2: Store the hyperparameters \mathbf{h}^t of $\mathcal{GP}(\mathcal{D}^t)$ into $\mathcal{H} = \{\mathbf{h}^t\}_{t=1}^{T-1}$.

Step 3: Use the classic k -means clustering algorithm to divide \mathcal{H} into $k > 1$ clusters.

Step 4: For each cluster, pick up the hyperparameters closest to its centroid and the corresponding dataset is chosen as a source data.

Remark 3. In this paper, we use the hyperparameters of $\mathcal{GP}(\mathcal{D}^t)$ as the implicit features to represent the characteristics of the problem landscape of $f(\mathbf{x}, t)$ where $t \in \{1, \dots, T-1\}$.

Remark 4. In practice, it is not necessary to build all $T-1$ GPR models from scratch in Step 1 and Step 2 each time. Instead, we only need to build the GPR model for the previous time step at the outset of each new optimization task.

Remark 5. To facilitate the knowledge transfer and to mitigate the potential negative transfer, a common idea for source task selection, widely studied in the transfer learning and multi-task learning literature [61], is to identify the most similar task(s). However, in the context of dynamic optimization, we can hardly obtain enough data at the outset of the new time step. This thus largely leads to some unexpected bias if we still try to align the previous tasks with the underlying one. Bearing this consideration in mind, the basic idea of our proposed adaptive source data selection is to find the most representative tasks to serve our purpose.

Let us use the example in Fig. 2 and Fig. 3 to illustrate this process. As shown in Fig. 2, by using the k -means clustering algorithm, the hyperparameters (note that $\bar{\ell}$ is normalized ℓ within the

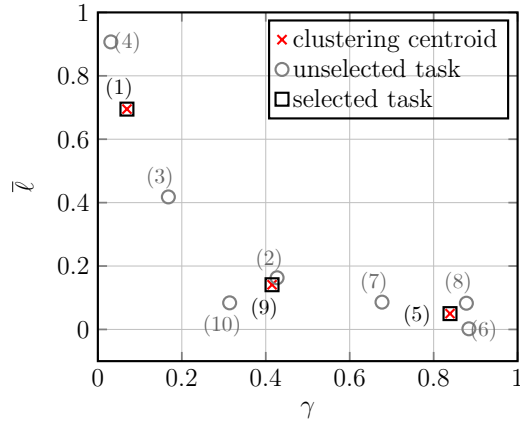


Figure 2: An illustrative example of the adaptive source data selection w.r.t. the hyperparameters of the RBF kernel in HGP for the moving peak problem at 10 different time steps. Here we set $k = 3$ in the k -means clustering. The selected tasks are denoted as the black \square symbol while the unselected tasks are denoted as the gray \circ symbol.

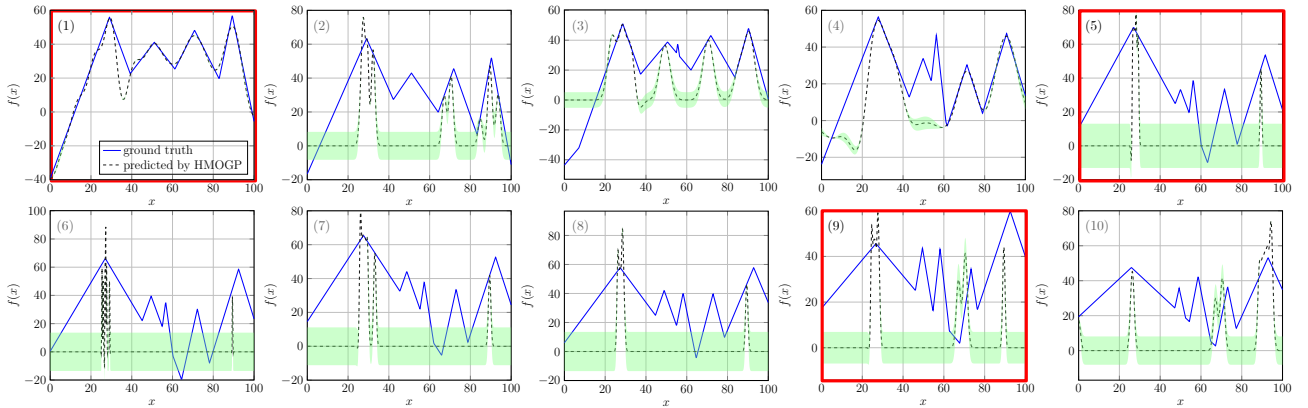


Figure 3: An illustrative example of the fitness landscapes (including both the ground truth versus the prediction made by the corresponding HMOGP) of the moving peak problems at 10 different time steps. The selected tasks are highlighted with the **red bold frames**.

range $[0, 1]$) of 10 GPR models built by different source datasets are grouped into 3 clusters. By cross referencing to the fitness landscapes estimated by the corresponding GPR models in Fig. 3, we find that $\{\mathcal{D}^1, \mathcal{D}^3, \mathcal{D}^4\}$, $\{\mathcal{D}^5, \mathcal{D}^6, \mathcal{D}^7, \mathcal{D}^8\}$ and $\{\mathcal{D}^2, \mathcal{D}^9, \mathcal{D}^{10}\}$ bear much resemblance to each other within the same cluster whereas they complement the other tasks lying in a different cluster.

3.3 Warm Starting Initialization Mechanism

In the conventional BO and SAEA, the initialization step is usually implemented by an experimental design method that randomly samples a set of solutions in a strategic manner. However, given the potential recurrent patterns in DOP across different time steps, there should be some useful knowledge collected from the previous optimization tasks. It is counter-intuitive if such knowledge is ignored but just start the new problem-solving process from scratch. This is especially wasteful when considering an expensive optimization scenario in which the computational budget at each time step is highly limited. Bearing this consideration in mind, we develop a bespoke initialization mechanism that leverages the information of related previous tasks recommended by the adaptive source task selection to warm start the underlying optimization task. Specifically, it has the following two major steps.

Step 1: For each of the k tasks recommended by the adaptive source task selection discussed in Section 3.2, identify the set of local optima \mathcal{L}^i where $i \in \{1, \dots, k\}$ w.r.t. the corresponding GPR model.

Step 2: For each task $i \in \{1, \dots, k\}$, sort the samples in \mathcal{L}^i based on the predicted objective function values. Use the following three-step procedure to pick up $1 \leq \sigma < |\mathcal{L}^i|$ samples to constitute the augmented dataset \mathcal{A}^i (started from an empty set) for the i -th task.

Step 2.1: Pick up the current best sample and calculate its Euclidean distance(s) w.r.t. all samples in \mathcal{A}^i .

Step 2.2: If any of the distances is less than a threshold ϵ_ℓ , remove this sample from \mathcal{L}^i and we move to the next sample then go to Step 2.1. Otherwise, this sample is removed from \mathcal{L}^i and it is added into \mathcal{A}^i .

Step 2.3: Repeat Step 2.1 and Step 2.2 until the size of \mathcal{A}^i reaches σ .

Remark 6. *Since the GPR model is continuously differentiable, we can derive the first order derivative of the predicted mean function w.r.t. a solution \mathbf{x} as:*

$$\frac{\partial \bar{g}(\mathbf{x})}{\partial \mathbf{x}} = \frac{\partial \mathbf{k}^*}{\partial \mathbf{x}} K^{-1} \mathbf{f}. \quad (13)$$

Based on the KKT conditions in Theorem 1 and equation (13), we can derive the saddle points of the corresponding GPR model by identifying the solutions that satisfy $\frac{\partial \mathbf{k}^}{\partial \mathbf{x}} K^{-1} \mathbf{f} = 0$. They are thereafter used as the local optima in Step 1.*

Remark 7. *Instead of re-evaluating the objective function values of the selected samples in \mathcal{A}^i where $i \in \{1, \dots, k\}$, we only use the corresponding GPR model to assign a pseudo objective function value to each sample.*

Remark 8. *In Step 2, a naïve idea is to pick the top σ samples from \mathcal{L}^i where $i \in \{1, \dots, k\}$. However, it can be less representative if the selected local optima are crowded within a small niche. Thus, we try to enforce certain level of diversity by making sure that the inter distance of samples in \mathcal{A}^i is at least larger than $\epsilon_\ell = 10^{-2} \times \max_{1 \leq i \leq n} (x_i^U - x_i^L)$.*

3.4 Optimization of Acquisition Function by a Hybrid EA

As discussed in [62], the optimization of UCB is non-trivial given its non-convex properties. In view of the outstanding performance of differential evolution (DE) [63] for global optimization, here we propose a simple but effective DE variant with local search to serve a proof-of-concept purpose. Specifically, it consists of the following six steps.

Step 1: Initialize a population of solutions $\mathcal{P} = \{\mathbf{x}^i\}_{i=1}^N$.

Step 2: Use DE to generate a population of offspring \mathcal{Q} and let $\bar{\mathcal{P}} = \mathcal{P} \cup \mathcal{Q}$.

Step 3: Pick up the best κ candidates from $\bar{\mathcal{P}}$, according to the UCB value, to constitute an archive $\bar{\mathcal{A}}$.

Step 4: For each candidate $\tilde{\mathbf{x}} \in \bar{\mathcal{A}}$ do

Step 4.1: Use stochastic gradient descent (SGD) [64] on $\tilde{\mathbf{x}}$ to obtain $\tilde{\mathbf{x}}^*$, then set $\bar{\mathcal{P}} = \bar{\mathcal{P}} \cup \{\tilde{\mathbf{x}}^*\} \setminus \{\tilde{\mathbf{x}}\}$.

Step 4.2: If $\|\tilde{\mathbf{x}}^* - \tilde{\mathbf{x}}\|_2 < \epsilon_d$, then set $\kappa = \max(\kappa - 1, 1)$; otherwise, set $\kappa = \min(\kappa + 1, 2N)$.

Step 5: Pick up the best N solutions from $\bar{\mathcal{P}}$ to constitute \mathcal{P} according to their UCB values.

Step 6: If the termination criterion is met, then stop and output $(\mathbf{x}^*, t) = \operatorname{argmax}_{\mathbf{x} \in \mathcal{P}} f^{\text{acq}}(\mathbf{x})$. Otherwise, go to Step 2.

Remark 9. *This DE variant leverages the global search ability of the DE and the local search characteristics of the SGD to achieve a balance between exploration and exploitation.*

Remark 10. κ is a prescribed hyperparameter that controls the scale of the local search. In this paper, we set $\kappa = 5$ in the initialization, i.e., Step 1, while it will be adaptively tuned in Step 4.2.

Remark 11. In Step 4.2, if $\tilde{\mathbf{x}}^*$ is very similar to $\tilde{\mathbf{x}}$, i.e., their Euclidean distance (denoted as $\|\cdot\|_2$) is smaller than a threshold ϵ_d , it implies the local search might not be helpful any longer. Therefore, κ will be reduced in the next round.

4 Experimental Setup

In this section, we introduce the experimental settings for validating the effectiveness of our proposed DETO compared against nine peer algorithms.

4.1 Benchmark Test Problems

In our experiments, we consider two synthetic benchmark problems. One is the moving peaks benchmark (MPB) [65], the most popular benchmark test suite in the dynamic optimization literature. MPB generates a landscape that consists of several components. Each component has a peak whose height, width and location change over time with the environment changes. MPB is flexible and can generate scalable functions with a configurable number of components, each of which is able to become the global optimum at the current time step. In addition, we develop another synthetic benchmark problem based on the MPB, named MPB with Gaussian peaks (MPBG). It is featured with Gaussian peaks while the other characteristics are kept the same. The mathematical definitions and visual interpretations of the fitness landscapes of both MPB and MPBG can be found in the Appendix A of the supplemental document of this paper¹.

4.2 Peer Algorithms

The differences of nine selected peer algorithms versus our proposed DETO are outlined as follows.

- Restart BO (RBO): This is the vanilla BO that restarts from scratch when the environment changes.
- Continuous BO (CBO): Different from RBO, it ignores the time-varying nature of DOP but applies all data collected so far in \mathcal{D} to train a GP model. In view of the cubic complexity of training and inference of GP, CBO can be excessively time consuming with the increase of time steps in our dynamic optimization setting. To mitigate this issue, we only consider the most recent five time steps in our experiments.
- Discounted information via noise sampling (DIN) [13]: This is best variant reported in [13] for tracking the varying global optimum in dynamic environments. It augments a noise term as a function of the age of the samples into the covariance function of GP.
- Model-based optimization (MBO) [15]: Instead of using the previously collected data in model training, MBO proposed an augmented acquisition function to search for the next point of merit.
- Time varying GP bandit optimization (TV-GP-UCB) [66]: It is an extension of the classical GP upper confidence bound algorithm [9]. To dump old and irrelevant data in a smooth fashion, it aggregates a decaying factor into a spatial-temporal kernel.
- BO with box mechanism (Box+GP) [67]: Instead of searching from a set of arbitrarily defined search ranges, it automatically designs the BO search space geometries by relying on previous FEs. This strategy endows the existing BO methods with transfer learning properties.
- Ranking-weighted GP ensemble (RGPE) [68]: It develops an ensemble model for BO by aggregating GPs built from previously collected data as a linear combination. In particular, the weights are learned in a transfer learning setting based on agnostic Bayesian learning of ensembles.

¹The supplemental document is located in <https://tinyurl.com/c2nd64ar>.

- Boosted hierarchical GP (BHGP) [69]: By using an ad-hoc independent assumption between the source and target data, it develops a boosted version of hierarchical GP to speed up BO from a transfer learning perspective.
- Transfer BO (TBO) [17]: It uses a MOGP to leverage the information collected from the previous time steps. In addition, a simple decay mechanism is applied to downgrade the impact of ‘older’ samples collected from the previous time steps.

4.3 Performance Metrics

Since the landscape and optimum change over time in DOP, it is not adequate to simply evaluate the quality of the best solution found by an algorithm in performance comparison. Instead, we need to take more information (e.g., how the algorithms track the moving optima) into account. In this paper, we consider the following two performance metrics.

- Average error overtime: it measures the average deviation from the global optimum over all FEs:

$$\bar{\epsilon}_f = \frac{1}{N_{\text{FE}}} \sum_{i=1}^{N_{\text{FE}}} \left[f(\mathbf{x}^*, t) - f_i(\bar{\mathbf{x}}^*, t) \right], \quad (14)$$

where N_{FE} is the total number of FEs, $f(\mathbf{x}^*, t)$ is the global optimum at the t -th time step, $t \in \{1, \dots, T\}$, and $f_i(\bar{\mathbf{x}}^*, t)$ is the best solution found at the i -th FE of the t -th time step.

- Average error for each time step: it measures the average accuracy achieved over all time steps:

$$\bar{\epsilon}_t = \frac{1}{T} \sum_{t=1}^T \left[f(\mathbf{x}^*, t) - f(\hat{\mathbf{x}}^*, t) \right], \quad (15)$$

where $f(\mathbf{x}^*, t)$ is the true global optimum at the t -th time step, $t \in \{1, \dots, T\}$, and $f(\hat{\mathbf{x}}^*, t)$ is the best solution found at the end of the t -th time step.

4.4 Statistical Tests

To have a statistical interpretation of the significance of comparison results, we use the following three statistical measures in our empirical study.

- Wilcoxon signed-rank test [70]: This is a non-parametric statistical test that makes little assumption about the underlying distribution of the data and has been recommended in many empirical studies in the EA community [71]. In particular, the significance level is set to $p = 0.05$ in our experiments.
- Scott-Knott test [72]: Instead of merely comparing the raw metric values, we apply the Scott-Knott test to rank the performance of different peer techniques over 31 runs on each test problem. In a nutshell, the Scott-Knott test uses a statistical test and effect size to divide the performance of peer algorithms into several clusters. The performance of peer algorithms within the same cluster are statistically equivalent. Note that the clustering process terminates until no split can be made. Finally, each cluster can be assigned a rank according to the mean metric values achieved by the peer algorithms within the cluster. In particular, the smaller the rank is, the better performance of the algorithm achieves.
- A_{12} effect size [73]: To ensure the resulted differences are not generated from a trivial effect, we apply A_{12} as the effect size measure to evaluate the probability that one algorithm is better than another. Specifically, given a pair of peer algorithms, $A_{12} = 0.5$ means they are *equivalent*. $A_{12} > 0.5$ denotes that one is better for more than 50% of the times. $0.56 \leq A_{12} < 0.64$ indicates a *small* effect size while $0.64 \leq A_{12} < 0.71$ and $A_{12} \geq 0.71$ mean a *medium* and a *large* effect size, respectively.

Note that both Wilcoxon signed-rank test and A_{12} effect size are also used in the Scott-Knott test for generating clusters.

4.5 Parameter Settings

The parameter settings used in our experiments are summarized as follows.

- Test problem settings: We consider different number of variables as $n \in \{3, 5, 8, 10\}$. The total number of peaks in MPB and MPBG is $m = 5$. In our experiments, we consider both small and large changes by setting the control parameters as $(\tilde{h} = 1.0, \tilde{s} = 1.0)$ and $(\tilde{h} = 5.0, \tilde{s} = 7.0)$ respectively.
- Computational budget: In our experiments, we consider $T = 10$ time steps in total and each time step is allocated with an extremely limited FEs. Specifically, $N_{\text{FE}} = 2 \times (11n - 1)$ at the first time step with $11n - 1$ for initial sampling. As for the follow up time steps, $N_{\text{FE}} = 9n$ of which $2n$ FEs are used for the initialization purpose.
- Parameters of peer algorithms: For DETO, the number of clusters $k = 3$, the scale of the local search $\kappa = 5$ and the closeness threshold $\epsilon_d = 0.01$. For DIN, $s^2 = 2.0$. For MB0, $c = 1.0$. For TV-GP-UCB, $\epsilon = 1/\sqrt{5}$.

5 Experimental Results

Our empirical study conducted in this section aims to answer the following research questions (RQs).

- RQ1: How is the performance of DETO compared against the other peer algorithms at different dimensions?
- RQ2: What is the effect brought by the significance of the change of environments?
- RQ3: What is the benefit of hierarchical version of MOGP versus the conventional LMC?
- RQ4: What is the benefit of the adaptive source data selection?
- RQ5: What is the benefit of the warm starting initialization mechanism?
- RQ6: What is the benefit of the hybrid DE with local search for the optimization of acquisition function?
- RQ7: How is the performance of DETO on solving a real-world problem in dynamic environments?

5.1 Performance Comparisons with Peer Algorithms

In this subsection, we investigate the performance comparison of our proposed DETO against the other peer algorithms.

5.1.1 Methods

To address RQ1 and RQ2, the results are presented from the following five aspects.

- First, the statistical comparison results on $\bar{\epsilon}_f$ and $\bar{\epsilon}_t$ are given in Tables 1 and 2.
- Then, we apply the A_{12} effect size to further understand the performance difference between DETO and the other peer algorithms on $\bar{\epsilon}_f$ and $\bar{\epsilon}_t$. Given the large amount of comparisons, we pull 9×16 results collected from A_{12} effect size together and calculate the percentage of different effect sizes obtained by a pair of dueling algorithms. These are presented as bar charts in Fig. 4.
- To have an overall comparison across different benchmark test problems, we apply the Scott-Knott test to rank the performance of different algorithms. To facilitate a better interpretation of many comparison results, we pull 9×16 comparison results collected from the Scott-Knott test together along with their variances as the bar charts with error bars in Fig. 5.

- To facilitate the understanding of the convergence rates of different algorithms during the dynamic optimization process, we develop two dedicated metrics as follows.

- First, we keep a record of the loss w.r.t. the corresponding optimum at a given FE as:

$$\mathcal{L}(\mathbf{x}, t) = f(\mathbf{x}^*, t) - f(\bar{\mathbf{x}}^*, t), \quad (16)$$

where $(\bar{\mathbf{x}}^*, t)$ is the best solution found at the corresponding FE of the t -th time step.

- The other metric evaluates the difference of the budget required by a peer algorithm w.r.t. the best algorithm at each time step. It is calculated as:

$$\rho_c = \frac{1}{T} \sum_{t=1}^T \frac{N_{\text{FE}}^t}{\tilde{N}_{\text{FE}}^{t*}}, \quad (17)$$

where $\tilde{N}_{\text{FE}}^{t*}$ is the number of FEs consumed by the best algorithm at the t -th time step to obtain its best solution $(\tilde{\mathbf{x}}^*, t)$. N_{FE}^t is the number of FEs required by one of the other peer algorithms to achieve $f(\tilde{\mathbf{x}}^*, t)$. Note that N_{FE}^t can be up to $8 \times N_{\text{FE}}$ in our experiments no matter whether the corresponding peer algorithm obtains $f(\tilde{\mathbf{x}}^*, t)$ or not. In practice, $\rho_c \geq 1$ and the larger ρ_c is, the worse the corresponding peer algorithm is.

- Last but not the least, we develop another metric ρ_t to investigate the effectiveness brought by the knowledge transfer, i.e., leveraging historical data from the previous optimization practice. It is calculated as:

$$\rho_t = \frac{1}{T} \sum_{t=1}^T \frac{N_{\text{FE}}^t}{N_c^t}, \quad (18)$$

where N_c^t is the number of FEs required by RBO, which completely ignores the historical data but restarts itself from scratch after each change, to obtain its best solution (\mathbf{x}_c^*, t) at the t -th time step. N_{FE}^t is the number of FEs required by one of the other peer algorithms that leverages historical information to a certain extent to achieve $f(\mathbf{x}_c^*, t)$. In practice, the corresponding knowledge transfer approach is regarded as effective when $0 < \rho_t < 1$ (the smaller ρ_t is, the better knowledge transfer is); otherwise it is negative to the underlying baseline optimization routine [74–76].

5.1.2 Results

Let us interpret the results according to the methods introduced in Section 5.1.1.

- From the comparison results on $\bar{\epsilon}_f$ and $\bar{\epsilon}_t$ shown in Tables 1 and 2, we can see that our proposed DETO is always the best algorithm in all comparisons without any exception. Note that all the better results are of statistical significance according to the Wilcoxon signed-rank test.
- In view of the overwhelmingly superior performance observed above, it is not surprised to see the stacked bar charts of A_{12} shown in Fig. 4 demonstrate that all the better comparison results achieved by DETO are always classified to be large.
- Likewise, based on the previous two comparison results, it is not difficult to infer the outstanding rank achieved by DETO according to the Scott-Knott test as shown in Figs. 5 and 6. In addition, we also notice that RBO, CBO, and Box+GP are the worst peer algorithms. As for RBO and CBO, their inferior performance is not surprising as ignoring any changes can hardly enable the BO to adapt to the new problem within a limited amount of FEs. Although Box+GP claimed to use a transfer learning approach to leverage the previous knowledge, its idea of shrinking search space is shown to be a mess when tackling the benchmark problems considered in our experiments. As the predecessor of DETO, the performance of TBO is competitive as it is ranked in the second place according to the Scott-Knott test. BHGP and RGPE also achieve a similar performance as TBO.

Table 1: Performance comparison results of $\bar{\epsilon}_f$ and $\bar{\epsilon}_t$ between DETO and the other 9 peer algorithms on the MPB problems

ϵ_t	$n=3$		$n=5$		$n=8$		$n=10$	
	$h=1.0, \bar{s}=1.0$	$h=5.0, \bar{s}=7.0$						
TBO-II	1.395E+1(6.51E+0)	2.000E+1(3.73E+0)	1.561E+1(1.22E+1)	2.628E+1(6.52E+0)	1.867E+1(9.86E+0)	2.476E+1(5.32E+0)	1.863E+1(1.10E+1)	2.211E+1(5.21E+0)
RBO	3.774E+1(2.00E+1) [†]	3.894E+1(1.28E+1) [†]	4.028E+1(1.95E+1) [†]	4.460E+1(1.03E+1) [†]	5.160E+1(2.84E+1) [†]	5.463E+1(1.47E+1) [†]	5.372E+1(1.98E+1) [†]	7.219E+1(1.74E+1) [†]
CBO	3.636E+1(1.32E+1) [†]	4.188E+1(1.45E+1) [†]	6.195E+1(1.90E+1) [†]	8.597E+1(2.41E+1) [†]	8.607E+1(2.90E+1) [†]	1.211E+2(2.44E+1) [†]	8.539E+1(3.23E+1) [†]	1.568E+2(5.36E+1) [†]
DIN	2.899E+1(1.05E+1) [†]	3.966E+1(1.23E+1) [†]	5.073E+1(2.74E+1) [†]	6.136E+1(2.06E+1) [†]	6.329E+1(2.75E+1) [†]	9.385E+1(3.44E+1) [†]	6.010E+1(1.68E+1) [†]	9.607E+1(2.07E+1) [†]
MBO	2.990E+1(1.74E+1) [†]	3.562E+1(1.60E+1) [†]	3.449E+1(1.76E+1) [†]	5.887E+1(1.27E+1) [†]	5.012E+1(6.63E+0) [†]	9.617E+1(3.82E+1) [†]	4.889E+1(1.43E+1) [†]	1.144E+2(4.58E+1) [†]
TV-GP-UCB	2.598E+1(9.58E+0) [†]	3.059E+1(8.46E+0) [†]	3.105E+1(1.92E+1) [†]	4.410E+1(1.41E+1) [†]	3.839E+1(1.73E+1) [†]	6.954E+1(3.12E+1) [†]	4.362E+1(1.81E+1) [†]	7.524E+1(3.11E+1) [†]
Box+GP	5.639E+1(1.49E+1) [†]	6.901E+1(1.90E+1) [†]	7.752E+1(2.44E+1) [†]	1.105E+2(3.48E+1) [†]	1.037E+2(3.32E+1) [†]	1.422E+2(3.98E+1) [†]	1.055E+2(3.84E+1) [†]	1.677E+2(4.70E+1) [†]
RGPE	2.041E+1(1.17E+1) [†]	2.125E+1(7.21E+0) [†]	2.580E+1(8.92E+0) [†]	3.012E+1(1.35E+1) [†]	2.870E+1(1.54E+1) [†]	3.570E+1(1.29E+1) [†]	2.806E+1(1.58E+1) [†]	4.271E+1(8.63E+0) [†]
BHGP	2.480E+1(1.41E+1) [†]	3.340E+1(1.20E+1) [†]	3.076E+1(1.81E+1) [†]	4.591E+1(1.22E+1) [†]	4.407E+1(1.88E+1) [†]	6.596E+1(3.26E+1) [†]	4.530E+1(1.52E+1) [†]	7.310E+1(1.62E+1) [†]
TBO	1.892E+1(8.17E+0) [†]	2.370E+1(1.02E+1) [†]	2.356E+1(1.57E+1) [†]	3.322E+1(1.01E+1) [†]	3.324E+1(1.57E+1) [†]	4.491E+1(1.97E+1) [†]	3.041E+1(8.52E+0) [†]	4.754E+1(2.23E+1) [†]

ϵ_f	$n=3$		$n=5$		$n=8$		$n=10$	
	$h=1.0, \bar{s}=1.0$	$h=5.0, \bar{s}=7.0$						
TBO-II	3.690E+1(1.59E+1)	4.191E+1(1.09E+1)	5.257E+1(1.80E+1)	5.669E+1(1.50E+1)	6.254E+1(2.60E+1)	6.918E+1(1.21E+1)	6.906E+1(2.30E+1)	7.647E+1(2.03E+1)
RBO	5.806E+1(1.65E+1) [†]	6.437E+1(2.10E+1) [†]	7.656E+1(3.48E+1) [†]	9.685E+1(3.05E+1) [†]	1.087E+2(5.82E+1) [†]	1.318E+2(3.32E+1) [†]	1.379E+2(4.30E+1) [†]	1.607E+2(2.31E+1) [†]
CBO	5.426E+1(1.92E+1) [†]	6.117E+1(1.07E+1) [†]	7.721E+1(3.17E+1) [†]	9.705E+1(2.21E+1) [†]	9.973E+1(4.16E+1) [†]	1.332E+2(3.22E+1) [†]	1.129E+2(3.62E+1) [†]	1.657E+2(4.01E+1) [†]
DIN	5.065E+1(1.97E+1) [†]	5.202E+1(1.69E+1) [†]	6.876E+1(3.03E+1) [†]	8.319E+1(1.93E+1) [†]	8.579E+1(4.21E+1) [†]	1.137E+2(2.86E+1) [†]	9.184E+1(3.16E+1) [†]	1.298E+2(2.74E+1) [†]
MBO	4.897E+1(1.91E+1) [†]	5.529E+1(1.39E+1) [†]	6.288E+1(2.47E+1) [†]	8.921E+1(2.16E+1) [†]	7.965E+1(3.96E+1) [†]	1.235E+2(3.84E+1) [†]	9.696E+1(2.48E+1) [†]	1.488E+2(3.98E+1) [†]
TV-GP-UCB	4.451E+1(1.19E+1) [†]	4.739E+1(1.42E+1) [†]	6.311E+1(2.59E+1) [†]	8.507E+1(2.35E+1) [†]	7.781E+1(3.31E+1) [†]	1.104E+2(3.40E+1) [†]	9.262E+1(3.16E+1) [†]	1.218E+2(1.98E+1) [†]
Box+GP	5.877E+1(1.74E+1) [†]	6.794E+1(2.04E+1) [†]	7.743E+1(3.04E+1) [†]	1.052E+2(3.08E+1) [†]	1.066E+2(5.20E+1) [†]	1.321E+2(3.10E+1) [†]	1.169E+2(3.67E+1) [†]	1.606E+2(4.08E+1) [†]
RGPE	4.032E+1(1.02E+1) [†]	4.503E+1(9.05E+0) [†]	5.412E+1(1.85E+1) [†]	6.937E+1(1.28E+1) [†]	6.950E+1(3.79E+1) [†]	8.776E+1(2.88E+1) [†]	7.709E+1(2.70E+1) [†]	1.065E+2(1.37E+1) [†]
BHGP	4.427E+1(1.16E+1) [†]	4.885E+1(1.13E+1) [†]	5.512E+1(2.23E+1) [†]	7.797E+1(1.97E+1) [†]	7.305E+1(3.44E+1) [†]	1.030E+2(3.02E+1) [†]	8.009E+1(2.54E+1) [†]	1.126E+2(3.51E+1) [†]
TBO	4.459E+1(1.33E+1) [†]	4.680E+1(1.29E+1) [†]	5.499E+1(1.98E+1) [†]	6.945E+1(1.33E+1) [†]	7.075E+1(3.52E+1) [†]	9.569E+1(2.97E+1) [†]	7.468E+1(2.32E+1) [†]	1.100E+2(2.48E+1) [†]

[†] indicates that DETO is significantly better than the corresponding peer algorithm according to the Wilcoxon signed-rank test at the 5% significance level.

Table 2: Performance comparison results of $\bar{\epsilon}_f$ and $\bar{\epsilon}_t$ between DETO and the other 9 peer algorithms on the MPBG problems

ϵ_t	$n=3$		$n=5$		$n=8$		$n=10$	
	$h=1.0, \bar{s}=1.0$	$h=5.0, \bar{s}=7.0$						
DETO	1.229E+1(1.27E+1)	1.328E+1(1.82E+1)	1.306E+1(1.98E+1)	2.286E+1(2.67E+1)	1.569E+1(1.80E+1)	2.217E+1(1.97E+1)	1.472E+1(2.26E+1)	2.042E+1(2.00E+1)
RBO	2.626E+1(3.73E+1) [†]	3.868E+1(3.93E+1) [†]	4.137E+1(5.89E+1) [†]	4.327E+1(4.11E+1) [†]	4.391E+1(4.72E+1) [†]	4.718E+1(4.67E+1) [†]	4.085E+1(4.49E+1) [†]	5.869E+1(6.02E+1) [†]
CBO	3.430E+1(3.91E+1) [†]	3.849E+1(3.77E+1) [†]	5.795E+1(6.15E+1) [†]	6.809E+1(7.42E+1) [†]	7.899E+1(7.60E+1) [†]	1.089E+2(1.05E+2) [†]	6.509E+1(7.33E+1) [†]	1.155E+2(1.49E+2) [†]
DIN	2.653E+1(2.50E+1) [†]	3.923E+1(3.66E+1) [†]	4.478E+1(5.39E+1) [†]	5.646E+1(4.99E+1) [†]	4.929E+1(5.46E+1) [†]	7.399E+1(8.28E+1) [†]	5.117E+1(5.06E+1) [†]	8.622E+1(8.05E+1) [†]
MBO	2.287E+1(2.89E+1) [†]	3.464E+1(3.48E+1) [†]	3.168E+1(3.95E+1) [†]	5.077E+1(4.95E+1) [†]	4.328E+1(4.65E+1) [†]	7.923E+1(9.40E+1) [†]	4.070E+1(3.75E+1) [†]	8.891E+1(1.01E+2) [†]
TV-GP-UCB	2.122E+1(2.48E+1) [†]	2.399E+1(2.74E+1) [†]	3.105E+1(3.81E+1) [†]	3.980E+1(4.04E+1) [†]	3.474E+1(3.85E+1) [†]	5.885E+1(7.33E+1) [†]	3.401E+1(4.15E+1) [†]	5.715E+1(6.56E+1) [†]
Box+GP	4.903E+1(5.13E+1) [†]	6.718E+1(5.90E+1) [†]	7.694E+1(8.72E+1) [†]	8.971E+1(9.42E+1) [†]	7.415E+1(9.97E+1) [†]	1.272E+2(1.12E+2) [†]	8.440E+1(7.96E+1) [†]	1.380E+2(1.45E+2) [†]
RGPE	1.301E+1(1.95E+1) [†]	2.115E+1(2.38E+1) [†]	2.509E+1(2.34E+1) [†]	2.568E+1(2.48E+1) [†]	2.212E+1(2.40E+1) [†]	3.191E+1(2.97E+1) [†]	2.105E+1(2.51E+1) [†]	3.948E+1(3.55E+1) [†]
BHGP	2.281E+1(2.46E+1) [†]	2.467E+1(3.23E+1) [†]	2.989E+1(4.04E+1) [†]	3.933E+1(4.08E+1) [†]	3.950E+1(4.64E+1) [†]	6.312E+1(6.84E+1) [†]	3.408E+1(3.99E+1) [†]	7.053E+1(6.06E+1) [†]
TBO	1.646E+1(2.10E+1) [†]	2.102E+1(2.62E+1) [†]	2.269E+1(2.98E+1) [†]	2.632E+1(3.14E+1) [†]	2.411E+1(2.98E+1) [†]	3.622E+1(4.18E+1) [†]	2.603E+1(2.70E+1) [†]	3.822E+1(4.19E+1) [†]

ϵ_f	$n=3$		$n=5$		$n=8$		$n=10$	
	$h=1.0, \bar{s}=1.0$	$h=5.0, \bar{s}=7.0$						
DETO	2.939E+1(3.42E+1)	3.911E+1(3.97E+1)	4.859E+1(5.30E+1)	5.281E+1(5.22E+1)	5.152E+1(6.43E+1)	6.505E+1(5.89E+1)	5.161E+1(6.12E+1)	6.830E+1(6.74E+1)
RBO	5.237E+1(5.67E+1) [†]	6.437E+1(6.41E+1) [†]	7.174E+1(9.41E+1) [†]	8.154E+1(8.67E+1) [†]	9.755E+1(1.23E+2) [†]	1.141E+2(1.12E+2) [†]	9.258E+1(1.22E+2) [†]	1.470E+2(1.35E+2) [†]
CBO	4.270E+1(4.87E+1) [†]	5.939E+1(5.05E+1) [†]	7.384E+1(9.02E+1) [†]	8.334E+1(7.84E+1) [†]	8.967E+1(1.03E+2) [†]	1.182E+2(1.11E+2) [†]	8.410E+1(1.05E+2) [†]	1.389E+2(1.45E+2) [†]
DIN	3.856E+1(4.84E+1) [†]	5.123E+1(5.21E+1) [†]	6.186E+1(8.30E+1) [†]	7.142E+1(6.81E+1) [†]	7.378E+1(8.52E+1) [†]	9.997E+1(9.76E+1) [†]	7.496E+1(8.31E+1) [†]	1.187E+2(1.05E+2) [†]
MBO	3.826E+1(4.39E+1) [†]	5.282E+1(4.87E+1) [†]	6.069E+1(7.79E+1) [†]	7.410E+1(7.02E+1) [†]	7.101E+1(8.07E+1) [†]	1.133E+2(1.10E+2) [†]	7.135E+1(8.00E+1) [†]	1.296E+2(1.28E+2) [†]
TV-GP-UCB	3.989E+1(4.17E+1) [†]	4.263E+1(4.50E+1) [†]	5.938E+1(7.07E+1) [†]	7.374E+1(7.15E+1) [†]	7.387E+1(7.75E+1) [†]	1.096E+2(1.12E+2) [†]	7.082E+1(8.68E+1) [†]	1.144E+2(9.82E+1) [†]
Box+GP	5.116E+1(5.03E+1) [†]	6.404E+1(6.17E+1) [†]	7.703E+1(9.24E+1) [†]	8.417E+1(9.01E+1) [†]	8.236E+1(1.04E+2) [†]	1.269E+2(1.07E+2) [†]	8.490E+1(9.83E+1) [†]	1.322E+2(1.34E+2) [†]
RGPE	3.256E+1(3.36E+1) [†]	4.272E+1(4.08E+1) [†]	5.047E+1(6.82E+1) [†]	5.910E+1(5.85E+1) [†]	6.088E+1(7.68E+1) [†]	7.478E+1(7.77E+1) [†]	6.000E+1(6.64E+1) [†]	9.888E+1(8.66E+1) [†]
BHGP	3.666E+1(3.98E+1) [†]	4.669E+1(4.77E+1) [†]	5.432E+1(6.32E+1) [†]	6.923E+1(6.90E+1) [†]	6.881E+1(7.95E+1) [†]	9.749E+1(1.00E+2) [†]	6.336E+1(7.37E+1) [†]	1.041E+2(9.08E+1) [†]
TBO	3.618E+1(3.76E+1) [†]	4.307E+1(4.57E+1) [†]	5.231E+1(6.55E+1) [†]	6.502E+1(5.41E+1) [†]	5.808E+1(7.59E+1) [†]	8.284E+1(8.41E+1) [†]	5.875E+1(6.07E+1) [†]	9.955E+1(9.96E+1) [†]

[†] indicates that DETO is significantly better than the corresponding peer algorithm according to the Wilcoxon signed-rank test at the 5% significance level.

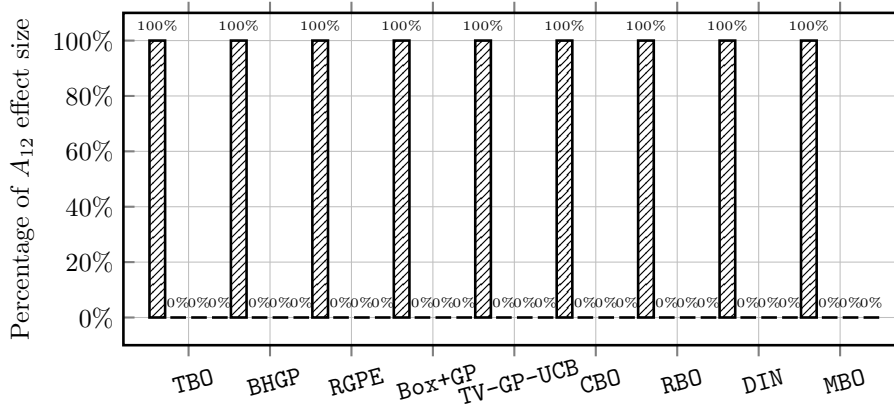


Figure 4: Percentage of the large, medium, small, and equal A_{12} effect size of $\bar{\epsilon}_f$ and $\bar{\epsilon}_t$ when comparing DETO with the other nine peer algorithms.

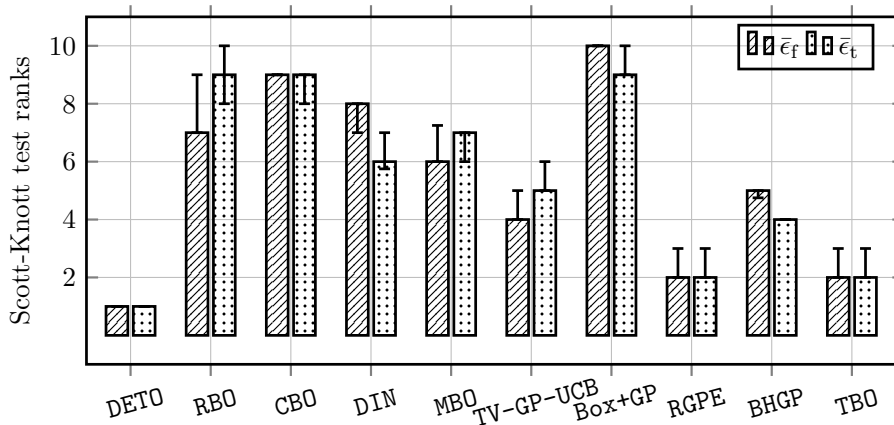


Figure 5: Bar charts with error bars of Scott-Knott test ranks of $\bar{\epsilon}_f$ and $\bar{\epsilon}_t$ achieved by each of the ten algorithms (the smaller rank is, the better performance achieves).

DETO	1.3	1.3	1.2	1.6	1.8	1.7	1.1	1.0	1.3	1.4	1.4	1.9	1.8	1.8	1.0	1.0
RBO	8.4	7.4	6.9	6.6	7.1	5.0	4.3	4.6	8.2	7.6	7.0	7.0	6.8	4.6	4.0	4.9
CBO	7.8	8.8	9.3	9.1	7.5	8.8	9.0	9.2	8.0	8.8	9.1	9.1	8.2	9.0	8.8	9.3
DIN	6.1	7.5	7.1	7.6	7.2	7.7	6.7	6.8	6.0	7.1	6.9	7.6	7.4	7.7	6.8	6.7
MBO	6.3	5.4	6.0	5.7	6.4	6.6	7.6	7.6	6.1	5.6	5.8	5.1	5.9	6.7	7.6	7.9
TV-GP-UCB	5.1	4.7	4.2	4.6	4.5	4.9	5.3	5.4	5.4	5.0	4.0	4.9	4.7	5.1	5.7	4.7
BoxGP	10.0	9.9	9.6	9.8	10.0	10.0	9.9	9.6	10.0	9.9	9.9	9.9	10.0	10.0	10.0	9.7
RGPE	2.5	2.2	2.2	2.5	2.1	2.4	2.1	2.3	2.4	2.4	2.0	2.3	2.1	2.0	2.2	2.3
BHGP	4.4	4.9	5.3	5.2	5.4	5.3	5.8	5.5	4.4	4.9	5.7	5.0	5.1	5.6	6.0	5.4
TBO	3.0	2.8	3.2	2.4	3.1	2.6	3.2	3.0	3.0	2.3	3.2	2.2	3.0	2.4	3.0	3.1
	3	5	8	10	3	5	8	10	3	5	8	10	3	5	8	10
	$\bar{h} = 1.0, \bar{s} = 1.0$				$\bar{h} = 5.0, \bar{s} = 7.0$				$\bar{h} = 1.0, \bar{s} = 1.0$				$\bar{h} = 5.0, \bar{s} = 7.0$			
	MPB				MPB				MPBG				MPBG			

Figure 6: Heatmap of a breakdown of the average Scott-Knott test ranks achieved by ten algorithms (the smaller rank with a lighter cell is, the better performance achieves).

- From the selected trajectories of $\mathcal{L}(\mathbf{x}, t)$ shown in Figs. 7 and 8 while full results are provided in Figs. 3 and 4 in the Appendix B of the supplemental document, we can see that the performance DETO is close to the other nine peer algorithms at the first time step. This makes sense because

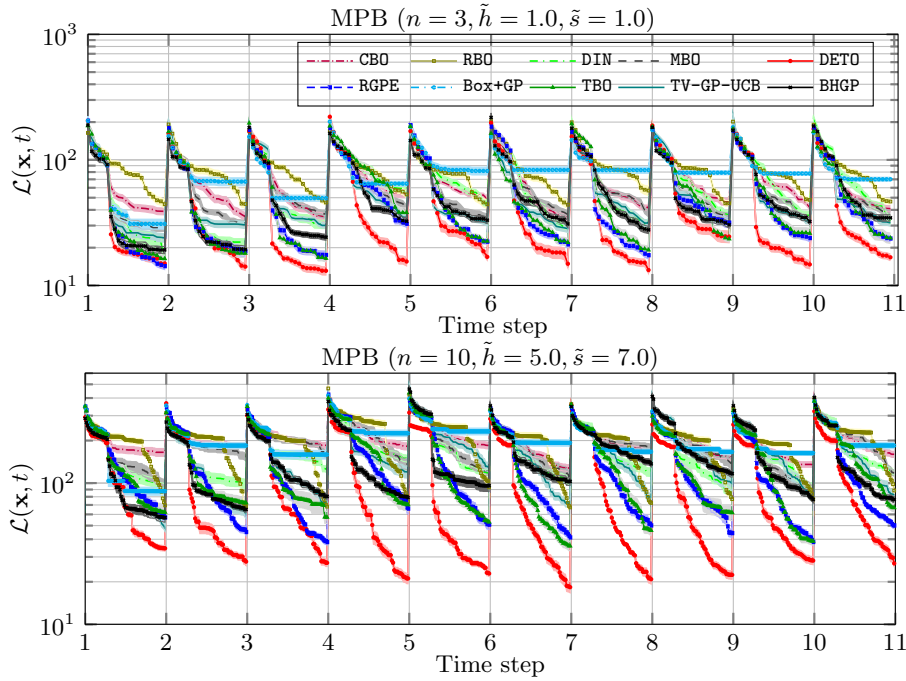


Figure 7: Trajectories of $\mathcal{L}(\mathbf{x}, t)$ with confidence bounds over $T = 10$ time steps achieved by ten algorithms on two selected MPB instances.

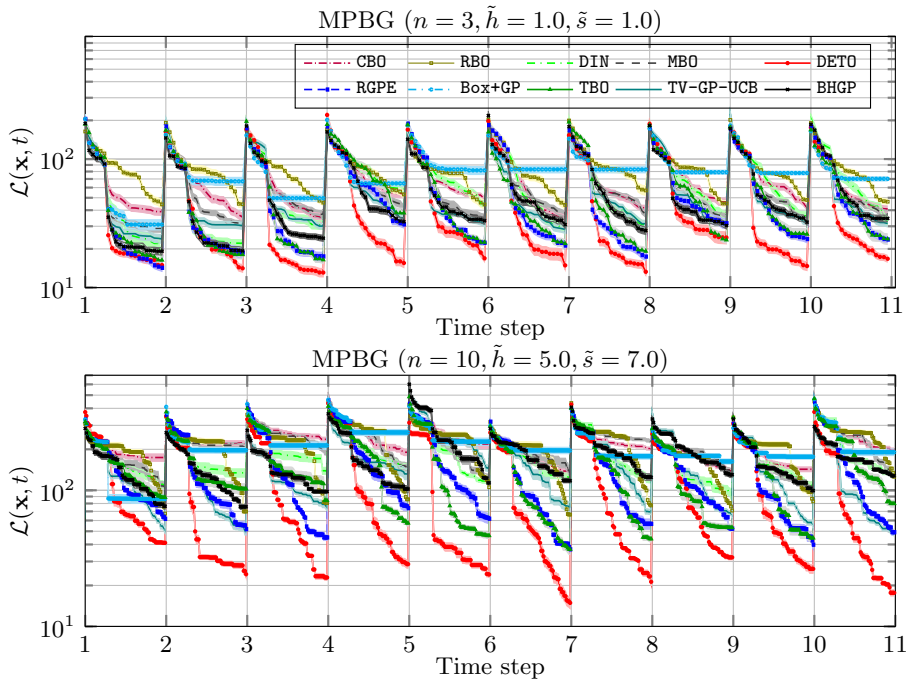


Figure 8: Trajectories of $\mathcal{L}(\mathbf{x}, t)$ with confidence bounds over $T = 10$ time steps achieved by ten algorithms on two selected MPBG instances.

there is no previous data available for DETO, whereas we observe a clear jump start since the second time step. This can be attributed to the effectiveness of leveraging ‘knowledge’ collected from the previous optimization practices. Although the other peer algorithms, except RBO and CBO, claimed to have a strategy to transfer knowledge from the historic data, they are not as effective as DETO. This might be because these algorithms are not specifically designed for dynamic optimization of which the problem changes overtime. Since only a limited amount of data are collected at each time step, they are not adequate to train a good model [77–79].

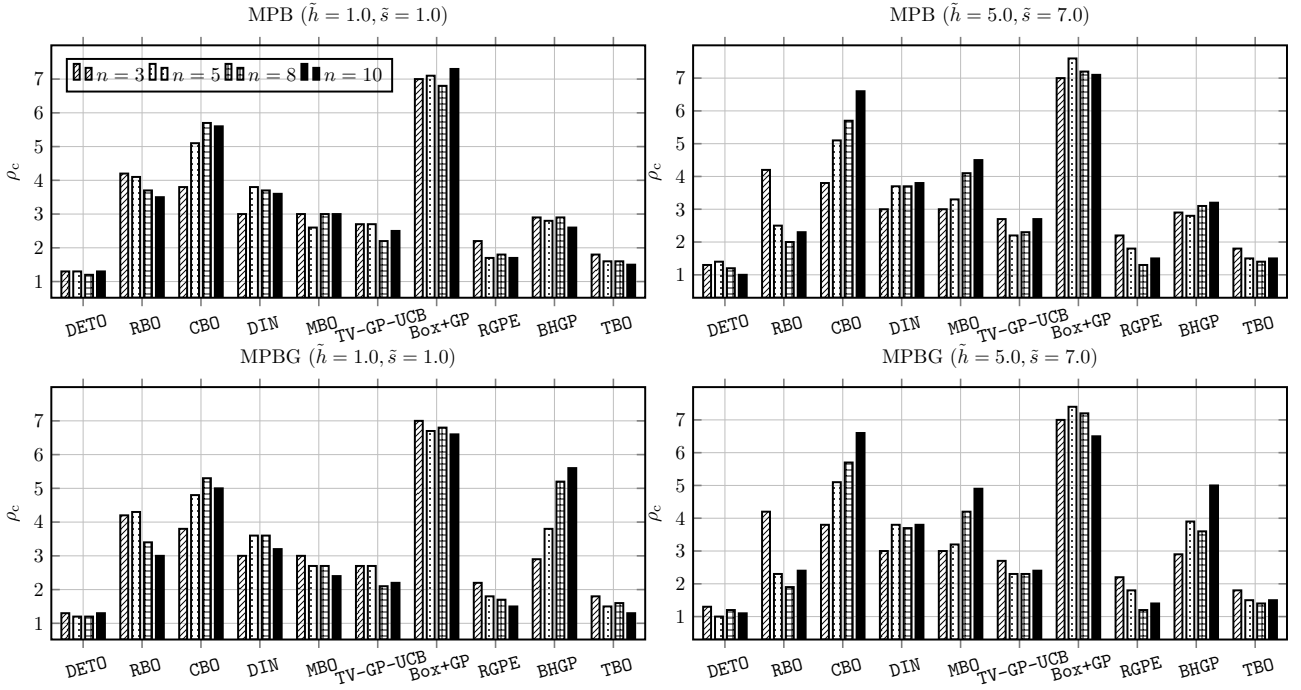


Figure 9: Bar charts of ρ_c obtained by DETO and the other nine peer algorithms.

- As the bar charts of ρ_c shown in Fig. 9, we can see that DETO is still the best algorithm. However, its superiority is not as overwhelming as those evaluated by the $\bar{\epsilon}_f$ and $\bar{\epsilon}_t$. The ρ_c obtained by TBO and RGPE are also close to 1.0, which means they can catch up with DETO when being allocated with reasonably more FEs. It is interesting to note that RBO is competitive where it even converges faster than some BO variants, especially **Box+GP**, the worst algorithm in all comparisons.
- The bar charts of ρ_t shown in Fig. 10 demonstrate the effectiveness of the knowledge transfer approaches used in DETO, TBO, and RGPE. In particular, DETO can be one time faster than RBO to achieve its comparable result. On the other hand, the performance of CBO is worse than RBO. This implies that simply feeding all historical data for surrogate modeling can be detrimental to the data-driven optimization. In addition, the knowledge transfer approaches used in DIN, MBO, and BHGP can be negative when handling DOPs with large changes [80–96].

5.2 Ablation Study

In this subsection, we investigate the effectiveness of the four building blocks of DETO as introduced in Sections 3.1 to 3.4, respectively.

5.2.1 Methods

To address RQ3 to RQ4, we design the following four variants of DETO in this ablation study.

- To address the RQ3, we develop a variant, denoted as **DETO-v1**, that replaces the HMOGP with the conventional LMC in the surrogate modeling step.
- To address the RQ4, we develop the following three variants with different source selection mechanisms.
 - **DETO-v2**: it selects the k most recent sources, i.e., $\{\mathcal{D}^i\}_{i=t-k}^{t-1}$ where $t > k$, to build the HMOGP.
 - **DETO-v3**: it selects k sources whose hyperparameters of the corresponding GPR models closest to \mathbf{h}^t . In other words, the selected source data are supposed to be most similar to the current time step.

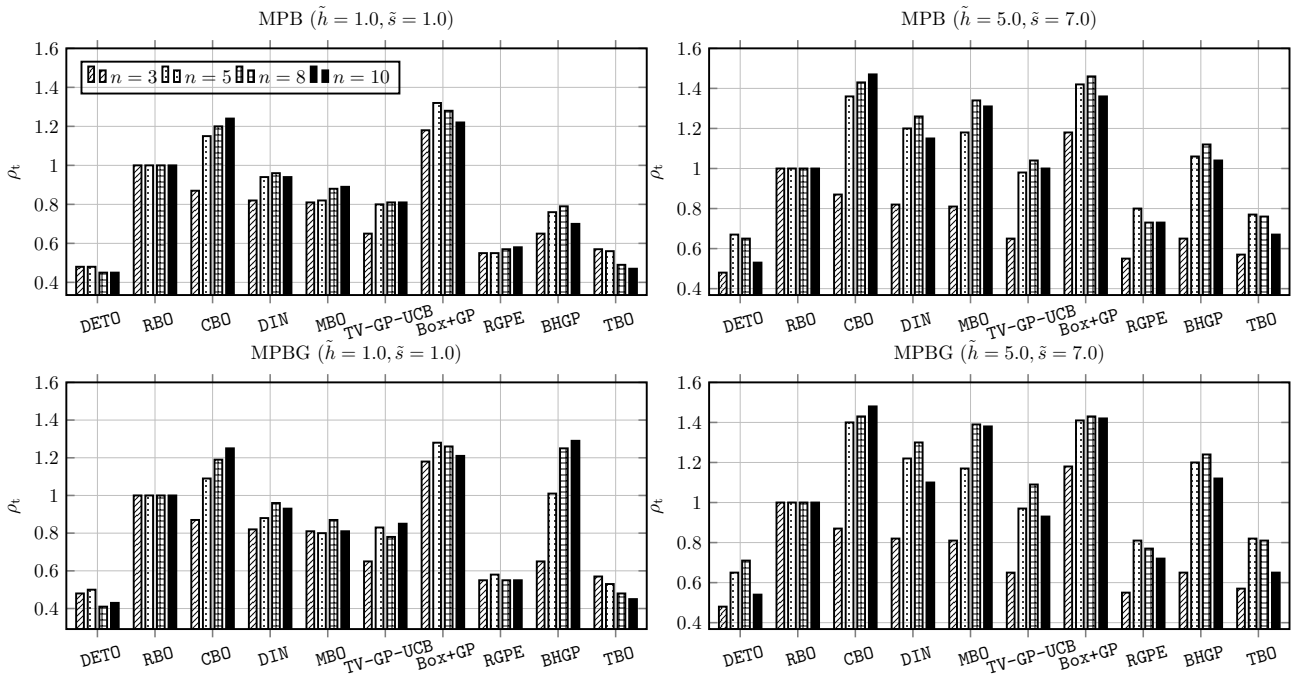


Figure 10: Bar charts of ρ_t obtained by DETO and the other nine peer algorithms.

– DETO-v4: it randomly selects k sources to serve the surrogate modeling purpose.

- To address the RQ5, we develop another variant DETO-v5 that replaces the warm starting initialization mechanism by a random initialization.
- To address the RQ6, we developed two variants DETO-v6 and DETO-v7 of which the hybrid DE with local search is replaced by a vanilla DE and a vanilla SGD, respectively.

5.2.2 Results

Let us interpret the results according to the methods introduced in Section 5.2.1

- From the comparison results of $\bar{\epsilon}_f$ and $\bar{\epsilon}_t$ shown in Tables I and II in the Appendix C of the supplemental document along with the 100% large A_{12} effect size shown in Fig. 11, we can see that a significant performance degradation of DETO when replacing the HMOGP with the conventional LMC. This is counter-intuitive at the first glance. Because the HMOGP can be treated as an approximation of the LMC with a significantly reduced order of hyperparameters, the LMC was supposed to be more expressive and have a more powerful modeling capability than the HMOGP. We attribute the inferior performance of DETO-v1 to the underfitting problem discussed in Section 3.1. Let us use an illustrative example of a MPB problem with $n = 1$ shown in Fig. 12 to elaborate this issue. As shown in this figure, both the LMC and the HMOGP work well when $t = 2$, i.e., the surrogate model is built by two data sets. However, the LMC becomes clearly underfit when $t = 5$ with a surprisingly high uncertainty estimation. It is even worse when $t = 10$. As discussed in Section 3.1, the hyperparameters of the LMC surges to 1,000 when $t = 10$ whereas the number of training data is way smaller. In contrast, the HMOGP performs consistently well even when $t = 10$ as its number of hyperparameters is merely 10, which is manageable [97–99].
- As the comparison results of $\bar{\epsilon}_f$ and $\bar{\epsilon}_t$ shown in Tables III and IV in the Appendix C of the supplemental document along with the A_{12} effect size shown in Fig. 13, we confirm that our proposed algorithm benefits from the adaptive source data selection mechanism. It is counter-intuitive to see that DETO-v3, which picks up the most similar k sources, is the worst variant. It is even outperformed by DETO-v4 which randomly selects k sources for surrogate modeling. This can be explained as the data collected during the initialization of each time step is not

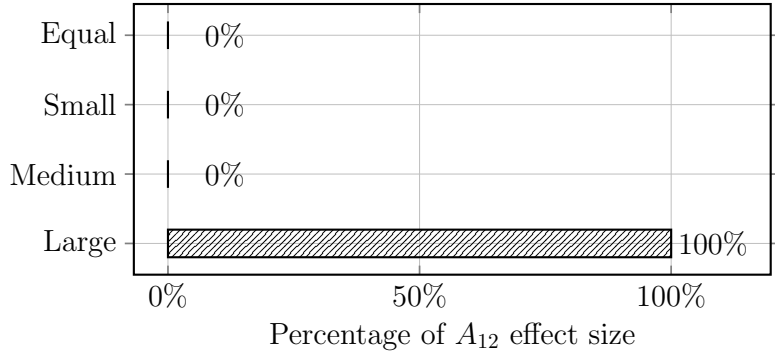


Figure 11: Percentage of the large, medium, small, and equal A_{12} effect size of $\bar{\epsilon}_f$ and $\bar{\epsilon}_t$ when comparing DETO with DETO-v1.

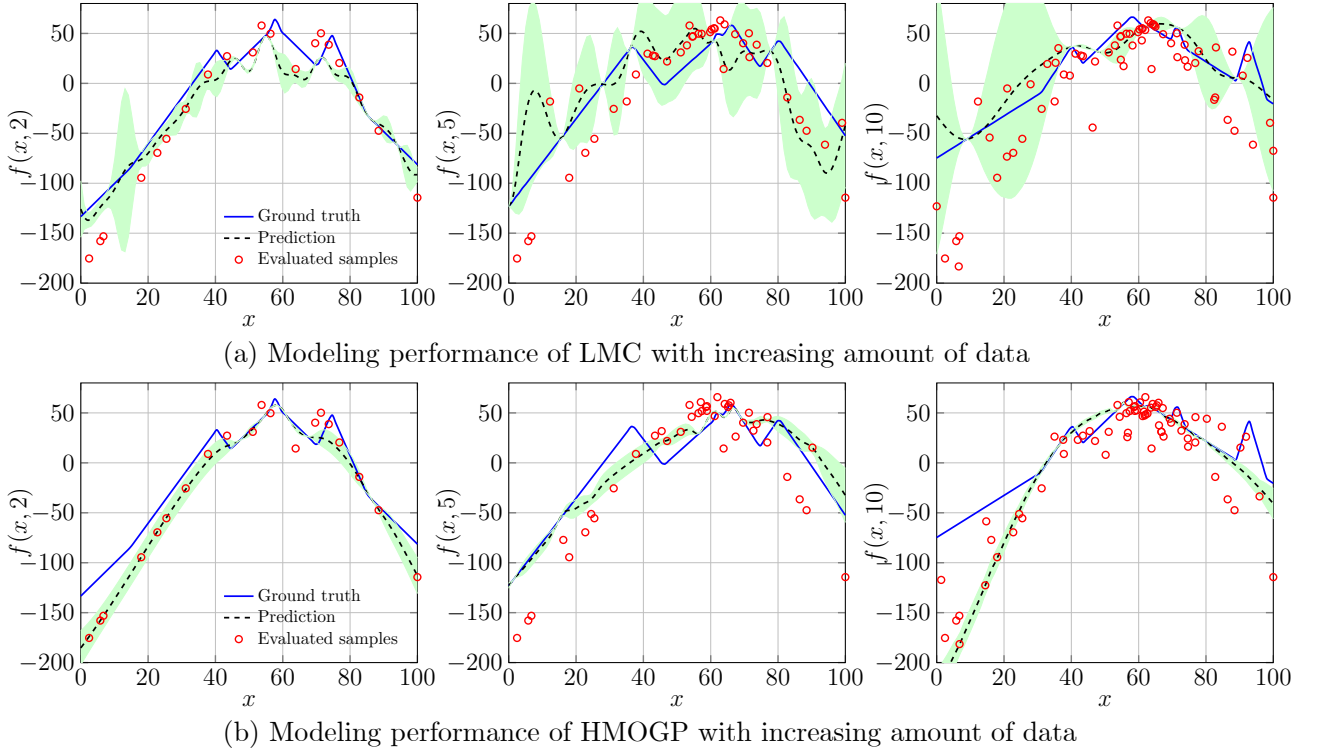


Figure 12: An illustrative example of underfitting problem of using the LMC versus the HMOGP for surrogate modeling of MPB problems.

sufficient to build a reasonably good surrogate model. Thus, choosing the similar source tasks can be misleading accordingly. It is interesting to note that the performance of DETO is close to that of DETO-v2 when $\tilde{h} = 1.0$ and $\tilde{s} = 1.0$, i.e., the dynamic problems with a small change. This can be explained as the landscape of such problem is close to its recent time steps, it makes sense to leverage the data collected from therein [100–119].

- From the comparison results of $\bar{\epsilon}_f$ and $\bar{\epsilon}_t$ shown in Tables V and VI in the Appendix C of the supplemental document along with the A_{12} effect size shown in Fig. 14, we can see the effectiveness of the warm starting initialization mechanism introduced in Section 3.3. However, it is also worth noting that the overwhelmingly better performance is diminishing when $n = 10$. This can be explained as the ineffectiveness of the surrogate modeling in a high-dimensional scenario with a strictly limited amount of training data. In this case, the local optima estimated from a less reliable model can be misleading [120–123].
- From the comparison results of $\bar{\epsilon}_f$ and $\bar{\epsilon}_t$ shown in Tables VII and VIII in the Appendix C of the supplemental document along with the A_{12} effect size shown in Fig. 13, we can see that our

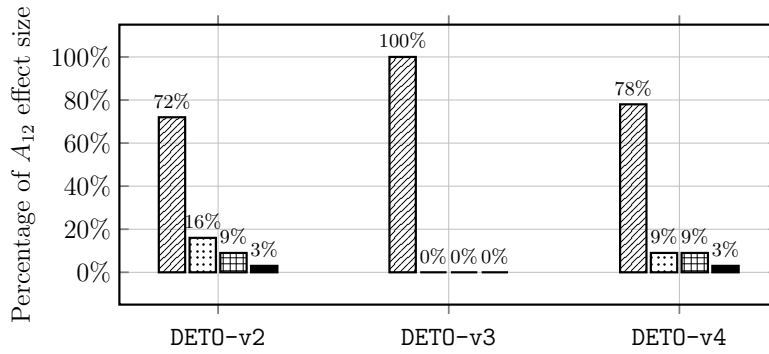


Figure 13: Percentage of the large, medium, small, and equal A_{12} effect size of $\bar{\epsilon}_f$ and $\bar{\epsilon}_t$ when comparing DETO with DETO-v2, DETO-v3, and DETO-v4.

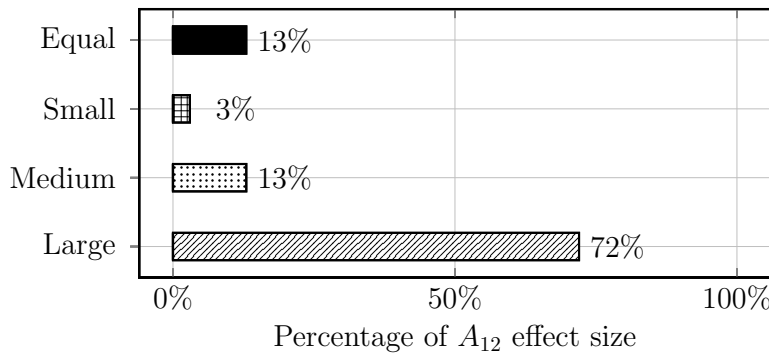


Figure 14: Percentage of the large, medium, small, and equal A_{12} effect size of $\bar{\epsilon}_f$ and $\bar{\epsilon}_t$ when comparing DETO with DETO-v5.

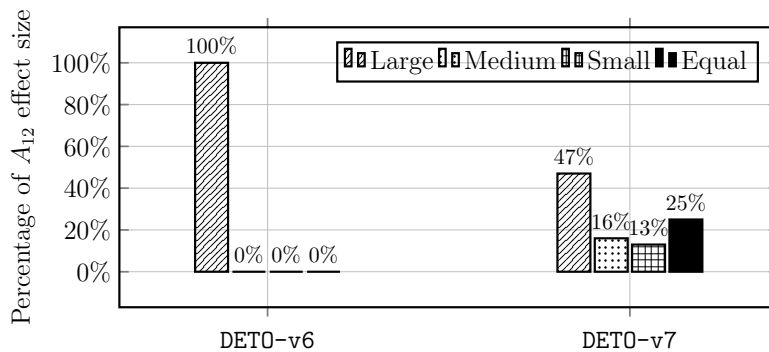


Figure 15: Percentage of the large, medium, small, and equal A_{12} effect size of $\bar{\epsilon}_f$ and $\bar{\epsilon}_t$ when comparing DETO with DETO-v6 and DETO-v7.

proposed hybrid DE with local search is the most effective optimizer for the acquisition function. Due to the non-convex property, neither vanilla DE nor SGD works well as both of them have a risk of being stuck at some local optima.

5.3 Real-World Dynamic Optimization

At the end, we validate the performance of DETO and the other nine peer algorithms on a real-world DOP of which the unknown objective function evolves over time. We consider here an automated machine learning task for handwritten digit recognition of the famous MNIST dataset [124]. As an illustrative example shown in Fig. 16, the digits are periodically rotated with time. Therefore, the hyperparameters associated with the baseline classifier, a multi-layer perceptron (MLP) in particular, need to be adjusted accordingly. The experimental settings are introduced as follows.

- In our experiments, we create 11 progressively changing datasets with 60,000 handwritten digit images for training and another 10,000 ones for testing. Each image has 28×28 pixels. In

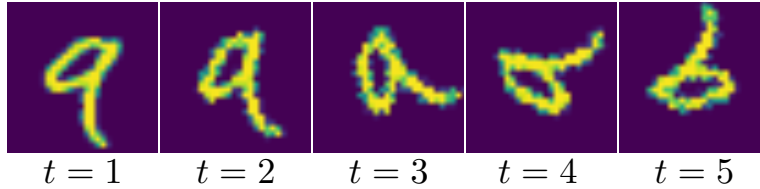


Figure 16: Illustrative example of the MNIST dataset with rotation at different time steps used in our experiments (detailed examples can be found in Fig. 5 of the Appendix D of the supplemental document).

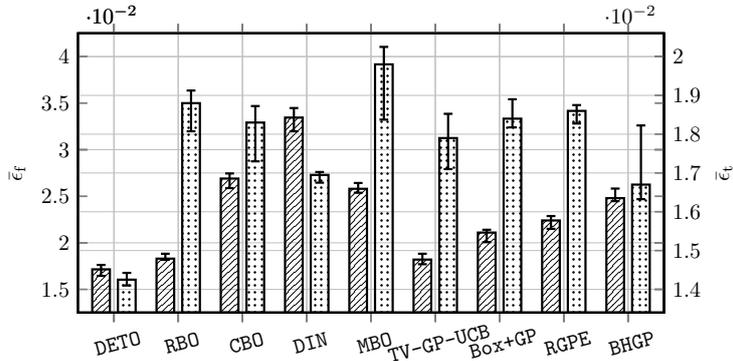


Figure 17: Bar charts with error bars of $\bar{\epsilon}_f$ and $\bar{\epsilon}_t$ achieved by DETO against the other nine peer algorithms on the real-world case study.

particular, to create dynamically changing scenarios, the images are rotated from 0° to 360° with a step size of 36° .

- We consider tuning four hyperparameters associated with the MLP outlined as below.
 - The number of neurons in the each hidden layer $n^h \in \{16, 32, 48, 64, 80, 96, 112, 128\}$.
 - The learning rate: $\alpha \in [10^{-6}, 1.0]$.
 - The momentum factor in SGD: $\beta \in [0.0, 1.0]$.
 - The weight for activation functions for the hidden layer $w \in [0.0, 1.0]$.

From the comparison results shown in Fig. 17, it is clear to see that our proposed DETO consistently outperforms the other peer algorithms on both $\bar{\epsilon}_f$ and $\bar{\epsilon}_t$ metrics. It is interesting to note that RBO is the second best algorithm on the $\bar{\epsilon}_f$ metric whereas it becomes the second worst one when considering the $\bar{\epsilon}_t$ metric. This observation implies that the transfer learning approaches used in other peer algorithms might lead to negative effect at the early stage of the hyperparameter optimization at each time step. Whereas a simple restarting from scratch is more robust at the early stage while its performance might be stagnated afterwards [125–128].

6 Conclusions

This paper develops a simple but effective data-driven transfer optimization framework that empowers data-driven evolutionary optimization to tackle expensive black-box optimization problems under dynamically changing environments. The main crux of our proposed DETO is a hierarchical MOGP as the surrogate model to implement a cost-effective knowledge transfer across the data collected from different time steps. In addition, an adaptive source task selection mechanism and a bespoke warm starting initialization strategy further enable a better knowledge transfer. In future, our proposed DETO framework can be extended from the following aspects.

- First, there has been a wealth of works on transfer learning in the literature [129]. In principle, any prevalent transfer learning approach can be applied in DETO in a plug-in manner. However, as discussed in Section 5.2, extra attention is required to mitigate the underfitting problems caused by the extremely limited computational budget allocated in DOPs.
- Meta-learning have been an emerging approach to learn new concepts and skills fast with a few training examples by a learning to learn paradigm [130]. It is promising to unleash the potential of meta-learning to tackle expensive DOPs under our proposed DETO framework.
- Last but not the least, existing transfer optimization approaches [131, 132] are hardly scalable to many tasks. However, real-world systems are usually designed to tackle a large number of (even infinitely many) problems over their lifetime. As one of our next ambitions, it is interesting to develop a life-long optimization paradigm that continuously learn knowledge from ongoing optimization practices and autonomously select useful information to new and unseen tasks in an open-ended environment.

Acknowledgment

This work was supported by UKRI Future Leaders Fellowship (MR/S017062/1), EPSRC (2404317), NSFC (62076056), Royal Society (IES/R2/212077) and Amazon Research Award.

References

- [1] R. Chen, K. Li, and X. Yao, “Dynamic multiobjectives optimization with a changing number of objectives,” *IEEE Trans. Evol. Comput.*, vol. 22, no. 1, pp. 157–171, 2018.
- [2] D. B. Fogel and Z. Michalewicz, *How to Solve It: Modern Heuristics*. Springer-Verlag Berlin Heidelberg, 2004.
- [3] C. E. Rasmussen and C. K. I. Williams, *Gaussian Processes for Machine Learning*. MIT Press, 2006.
- [4] M. L. Stein, *Interpolation of Spatial Data: Some Theory for Kriging*. Springer-Verlag New York, 1999.
- [5] T. J. Santner, B. J. Williams, and W. I. Notz, *The Design and Analysis of Computer Experiments*. Springer-Verlag New York, 2018.
- [6] D. R. Jones, “A taxonomy of global optimization methods based on response surfaces,” *J. Global Optimization*, vol. 21, no. 4, pp. 345–383, 2001.
- [7] P. I. Frazier, “A tutorial on Bayesian optimization,” 2018.
- [8] B. Shahriari, K. Swersky, Z. Wang, R. P. Adams, and N. de Freitas, “Taking the human out of the loop: A review of Bayesian optimization,” *Proc. IEEE*, vol. 104, no. 1, pp. 148–175, 2016.
- [9] N. Srinivas, A. Krause, S. M. Kakade, and M. W. Seeger, “Gaussian process optimization in the bandit setting: No regret and experimental design,” in *ICML’10: Proc. of the 27th International Conference on Machine Learning*. Omnipress, 2010, pp. 1015–1022.
- [10] D. R. Jones, M. Schonlau, and W. J. Welch, “Efficient global optimization of expensive black-box functions,” *J. Glob. Optim.*, vol. 13, no. 4, pp. 455–492, 1998.
- [11] Y. Jin, H. Wang, T. Chugh, D. Guo, and K. Miettinen, “Data-driven evolutionary optimization: An overview and case studies,” *IEEE Trans. Evol. Comput.*, vol. 23, no. 3, pp. 442–458, 2019.
- [12] K. Li and R. Chen, “Batched data-driven evolutionary multi-objective optimization based on manifold interpolation,” *IEEE Trans. Evol. Comput.*, 2022, accepted for publication.

- [13] S. Morales-Enciso and J. Branke, “Tracking global optima in dynamic environments with efficient global optimization,” *Eur. J. Oper. Res.*, vol. 242, no. 3, pp. 744–755, 2015.
- [14] F. M. Nyikosa, M. A. Osborne, and S. J. Roberts, “Bayesian optimization for dynamic problems,” 2018.
- [15] J. Richter, J. Shi, J. Chen, J. Rahnenführer, and M. Lang, “Model-based optimization with concept drifts,” in *GECCO’20: Proc. of 2020 Genetic and Evolutionary Computation Conference*. ACM, 2020, pp. 877–885.
- [16] X. Fan, K. Li, and K. C. Tan, “Surrogate assisted evolutionary algorithm based on transfer learning for dynamic expensive multi-objective optimisation problems,” in *CEC’20: Proc. of the 2020 IEEE Congress on Evolutionary Computation*. IEEE, 2020, pp. 1–8.
- [17] R. Chen and K. Li, “Transfer Bayesian optimization for expensive black-box optimization in dynamic environment,” in *SMC’21: Proc. of the 2021 IEEE Conference on Systems, Man, and Cybernetics*. IEEE, 2021, pp. 1374–1379.
- [18] M. Lindauer and F. Hutter, “Warmstarting of model-based algorithm configuration,” in *AAAI’18: Proc. of the Thirty-Second AAAI Conference on Artificial Intelligence*. AAAI Press, 2018, pp. 1355–1362.
- [19] H. Hu, J. Langford, R. Caruana, S. Mukherjee, E. Horvitz, and D. Dey, “Efficient forward architecture search,” in *NeurIPS’19: Proc. of the 32nd Annual Conference on Neural Information Processing Systems*, 2019, pp. 10 122–10 131.
- [20] M. A. Álvarez, L. Rosasco, and N. D. Lawrence, “Kernels for vector-valued functions: A review,” *Found. Trends Mach. Learn.*, vol. 4, no. 3, pp. 195–266, 2012.
- [21] D. P. Bertsekas, *Nonlinear Programming*. Athena Scientific; 3rd edition, 2016.
- [22] H. J. Kushner, “A versatile stochastic model of a function of unknown and time varying form,” *J. Math. Anal. Appl.*, vol. 5, pp. 150–167, 1962.
- [23] V. Perrone, R. Jenatton, M. W. Seeger, and C. Archambeau, “Scalable hyperparameter transfer learning,” in *NeurIPS’18: Proc. of 2018 Annual Conference on Neural Information Processing Systems*, 2018, pp. 6846–6856.
- [24] S. Flennerhag, P. G. Moreno, N. D. Lawrence, and A. C. Damianou, “Transferring knowledge across learning processes,” in *ICLR’19: Proc. of the 7th International Conference on Learning Representations*. OpenReview.net, 2019.
- [25] M. Wistuba, N. Schilling, and L. Schmidt-Thieme, “Scalable Gaussian process-based transfer surrogates for hyperparameter optimization,” *Mach. Learn.*, vol. 107, no. 1, pp. 43–78, 2018.
- [26] M. Volpp, L. P. Fröhlich, K. Fischer, A. Doerr, S. Falkner, F. Hutter, and C. Daniel, “Meta-learning acquisition functions for transfer learning in Bayesian optimization,” in *ICLR’20: Proc. of the 8th International Conference on Learning Representations*. OpenReview.net, 2020.
- [27] M. Wistuba, N. Schilling, and L. Schmidt-Thieme, “Two-stage transfer surrogate model for automatic hyperparameter optimization,” in *ECML/PKDD’16: Proc. of the 2016 European Conference on Machine Learning and Knowledge Discovery in Databases*, ser. Lecture Notes in Computer Science, vol. 9851. Springer, 2016, pp. 199–214.
- [28] N. Schilling, M. Wistuba, and L. Schmidt-Thieme, “Scalable hyperparameter optimization with products of Gaussian process experts,” in *ECML/PKDD’16: Proc. of the 2016 European Conference on Machine Learning and Knowledge Discovery in Databases*, ser. Lecture Notes in Computer Science, vol. 9851. Springer, 2016, pp. 33–48.

- [29] K. Swersky, J. Snoek, and R. P. Adams, “Multi-task Bayesian optimization,” in *NIPS’13: Proc. of the 27th Annual Conference on Neural Information Processing Systems*, 2013, pp. 2004–2012.
- [30] Y. Jin and J. Branke, “Evolutionary optimization in uncertain environments—a survey,” *IEEE Trans. Evol. Comput.*, vol. 9, no. 3, pp. 303–317, 2005.
- [31] T. T. Nguyen, S. Yang, and J. Branke, “Evolutionary dynamic optimization: A survey of the state of the art,” *Swarm Evol. Comput.*, vol. 6, pp. 1–24, 2012.
- [32] M. Mavrovouniotis, C. Li, and S. Yang, “A survey of swarm intelligence for dynamic optimization: Algorithms and applications,” *Swarm Evol. Comput.*, vol. 33, pp. 1–17, 2017.
- [33] D. Yazdani, R. Cheng, D. Yazdani, J. Branke, Y. Jin, and X. Yao, “A survey of evolutionary continuous dynamic optimization over two decades - part A,” *IEEE Trans. Evol. Comput.*, vol. 25, no. 4, pp. 609–629, 2021.
- [34] ———, “A survey of evolutionary continuous dynamic optimization over two decades - part B,” *IEEE Trans. Evol. Comput.*, vol. 25, no. 4, pp. 630–650, 2021.
- [35] H. G. Cobb and J. J. Grefenstette, “Genetic algorithms for tracking changing environments,” in *ICGA ’93: Proc. of the 5th International Conference on Genetic Algorithms*, 1993, pp. 523–530.
- [36] K. Deb, U. B. R. N., and S. Karthik, “Dynamic multi-objective optimization and decision-making using modified NSGA-II: A case study on hydro-thermal power scheduling,” in *EMO’07: Proc. of the 4th International Conference on Evolutionary Multi-Criterion Optimization*, vol. 4403. Springer, 2006, pp. 803–817.
- [37] T. T. Nguyen, “Continuous dynamic optimisation using evolutionary algorithms,” Ph.D. dissertation, University of Birmingham, 2011.
- [38] X. Hu and R. C. Eberhart, “Adaptive particle swarm optimization: Detection and response to dynamic systems,” in *CEC’02: Proc. of the 2002 Congress on Evolutionary Computation*, vol. 2, 2002, pp. 1–8.
- [39] S. Janson and M. Middendorf, “A hierarchical particle swarm optimizer for noisy and dynamic environments,” *Genet. Program. Evolvable Mach.*, vol. 7, no. 4, pp. 329–354, 2006.
- [40] J. M. M. Gouvêa and A. F. R. Araújo, “Evolutionary algorithm with diversity-reference adaptive control in dynamic environments,” *Int. J. Artif. Intell. Tools*, vol. 24, no. 1, pp. 1450013:1–1450013:36, 2015.
- [41] K. Li, S. Kwong, J. Cao, M. Li, J. Zheng, and R. Shen, “Achieving balance between proximity and diversity in multi-objective evolutionary algorithm,” *Inf. Sci.*, vol. 182, no. 1, pp. 220–242, 2012.
- [42] M. Mavrovouniotis and S. Yang, “Population-based incremental learning with immigrants schemes in changing environments,” in *SSCI’15: Proc. of 2015 IEEE Symposium Series on Computational Intelligence*. IEEE, 2015, pp. 1444–1451.
- [43] G. Ruan, G. Yu, J. Zheng, J. Zou, and S. Yang, “The effect of diversity maintenance on prediction in dynamic multi-objective optimization,” *Appl. Soft Comput.*, vol. 58, pp. 631–647, 2017.
- [44] J. L. Fernandez-Marquez and J. L. Arcos, “Adapting particle swarm optimization in dynamic and noisy environments,” in *CEC’10: Proc. of the IEEE Congress on Evolutionary Computation*. IEEE, 2010, pp. 1–8.
- [45] H. Cheng and S. Yang, “Genetic algorithms with immigrants schemes for dynamic multicast problems in mobile ad hoc networks,” *Eng. Appl. Artif. Intell.*, vol. 23, no. 5, pp. 806–819, 2010.

- [46] C. Li and S. Yang, “A general framework of multipopulation methods with clustering in undetectable dynamic environments,” *IEEE Trans. Evol. Comput.*, vol. 16, no. 4, pp. 556–577, 2012.
- [47] C. Li, T. T. Nguyen, M. Yang, S. Yang, and S. Zeng, “Multi-population methods in unconstrained continuous dynamic environments: The challenges,” *Inf. Sci.*, vol. 296, pp. 95–118, 2015.
- [48] C. Li, T. T. Nguyen, M. Yang, M. Mavrovouniotis, and S. Yang, “An adaptive multipopulation framework for locating and tracking multiple optima,” *IEEE Trans. Evol. Comput.*, vol. 20, no. 4, pp. 590–605, 2016.
- [49] A. S. Etaner-Uyar and A. E. Harmanci, “A new population based adaptive domination change mechanism for diploid genetic algorithms in dynamic environments,” *Soft Comput.*, vol. 9, no. 11, pp. 803–814, 2005.
- [50] S. Zhao and P. N. Suganthan, “Diversity enhanced particle swarm optimizer for global optimization of multimodal problems,” in *CEC’09: Proc. of the 2009 IEEE Congress on Evolutionary Computation*, 2009, pp. 590–597.
- [51] X. Peng, X. Gao, and S. Yang, “Environment identification-based memory scheme for estimation of distribution algorithms in dynamic environments,” *Soft Comput.*, vol. 15, no. 2, pp. 311–326, 2011.
- [52] M. Mavrovouniotis and S. Yang, “Direct memory schemes for population-based incremental learning in cyclically changing environments,” in *EvoApplications’16: Proc. of the 19th European Conference Applications of Evolutionary Computation*, 2016, pp. 233–247.
- [53] Z. Peng, J. Zheng, and J. Zou, “A population diversity maintaining strategy based on dynamic environment evolutionary model for dynamic multiobjective optimization,” in *CEC’14: Proc. of the 2014 IEEE Congress on Evolutionary Computation*, 2014, pp. 274–281.
- [54] I. Hatzakis and D. Wallace, “Dynamic multi-objective optimization with evolutionary algorithms: a forward-looking approach,” in *GECCO’06: Proc. of the 2006 Genetic and Evolutionary Computation Conference*, 2006, pp. 1201–1208.
- [55] A. Zhou, Y. Jin, and Q. Zhang, “A population prediction strategy for evolutionary dynamic multiobjective optimization,” *IEEE Trans. Cybern.*, vol. 44, no. 1, pp. 40–53, 2014.
- [56] Q. Zhang, S. Yang, S. Jiang, R. Wang, and X. Li, “Novel prediction strategies for dynamic multiobjective optimization,” *IEEE Trans. Evol. Comput.*, vol. 24, no. 2, pp. 260–274, 2020.
- [57] J. Zou, Q. Li, S. Yang, H. Bai, and J. Zheng, “A prediction strategy based on center points and knee points for evolutionary dynamic multi-objective optimization,” *Appl. Soft Comput.*, vol. 61, pp. 806–818, 2017.
- [58] C. Rossi, M. Abderrahim, and J. C. Díaz, “Tracking moving optima using Kalman-based predictions,” *Evol. Comput.*, vol. 16, no. 1, pp. 1–30, 2008.
- [59] A. Muruganantham, K. C. Tan, and P. Vadakkepat, “Evolutionary dynamic multiobjective optimization via kalman filter prediction,” *IEEE Trans. Cybern.*, vol. 46, no. 12, pp. 2862–2873, 2016.
- [60] S. Park and S. Choi, “Hierarchical Gaussian process regression,” in *ACML’20: Proc. of the 2nd Asian Conference on Machine Learning*, ser. JMLR Proceedings, vol. 13. JMLR.org, 2010, pp. 95–110.
- [61] F. Zhuang, Z. Qi, K. Duan, D. Xi, Y. Zhu, H. Zhu, H. Xiong, and Q. He, “A comprehensive survey on transfer learning,” *Proc. IEEE*, vol. 109, no. 1, pp. 43–76, 2021.

- [62] J. T. Wilson, F. Hutter, and M. P. Deisenroth, “Maximizing acquisition functions for bayesian optimization,” in *NeurIPS’18: Proc. of the 2018 Annual Conference on Neural Information Processing Systems 2018*, 2018, pp. 9906–9917.
- [63] R. Storn and K. V. Price, “Differential evolution - A simple and efficient heuristic for global optimization over continuous spaces,” *J. Glob. Optim.*, vol. 11, no. 4, pp. 341–359, 1997.
- [64] I. J. Goodfellow, Y. Bengio, and A. C. Courville, *Deep Learning*, ser. Adaptive computation and machine learning. MIT Press, 2016.
- [65] J. Branke, “Memory enhanced evolutionary algorithms for changing optimization problems,” in *CEC’99: Proc. of the 1999 Congress on Evolutionary Computation*, vol. 3, 1999, pp. 1875–1882.
- [66] I. Bogunovic, J. Scarlett, and V. Cevher, “Time-varying Gaussian process bandit optimization,” in *AISTATS’16: Proc. of the 19th International Conference on Artificial Intelligence and Statistics*, ser. JMLR Workshop and Conference Proceedings, vol. 51. JMLR.org, 2016, pp. 314–323.
- [67] V. Perrone and H. Shen, “Learning search spaces for Bayesian optimization: Another view of hyperparameter transfer learning,” in *NeurIPS’19: Proc. of the 2019 Annual Conference on Neural Information Processing Systems*, 2019, pp. 12 751–12 761.
- [68] M. Feurer, B. Letham, F. Hutter, and E. Bakshy, “Practical transfer learning for Bayesian optimization,” 2018. [Online]. Available: <https://arxiv.org/abs/1802.02219>
- [69] P. Tighineanu, K. Skubch, P. Baireuther, A. Reiss, F. Berkenkamp, and J. Vinogradska, “Transfer learning with Gaussian processes for Bayesian optimization,” in *AISTATS’22: Proc. of the 2022 International Conference on Artificial Intelligence and Statistics*, ser. Proceedings of Machine Learning Research, vol. 151. PMLR, 2022, pp. 6152–6181.
- [70] F. Wilcoxon, “Individual comparisons by ranking methods,” 1945.
- [71] J. Derrac, S. García, D. Molina, and F. Herrera, “A practical tutorial on the use of nonparametric statistical tests as a methodology for comparing evolutionary and swarm intelligence algorithms,” *Swarm Evol. Comput.*, vol. 1, no. 1, pp. 3–18, 2011.
- [72] N. Mittas and L. Angelis, “Ranking and clustering software cost estimation models through a multiple comparisons algorithm,” *IEEE Trans. Software Eng.*, vol. 39, no. 4, pp. 537–551, 2013.
- [73] A. Vargha and H. D. Delaney, “A critique and improvement of the CL common language effect size statistics of McGraw and Wong,” *J. Educ. Behav. Stat.*, vol. 25, no. 2, pp. 101–132, 2000.
- [74] L. Sun and K. Li, “Adaptive operator selection based on dynamic thompson sampling for MOEA/D,” in *PPSN’20: Proc. of the 16th International Conference on Parallel Problem Solving from Nature*, ser. Lecture Notes in Computer Science, vol. 12270. Springer, 2020, pp. 271–284.
- [75] H. Nie, H. Gao, and K. Li, “Knee point identification based on voronoi diagram,” in *SMC’20: Proc. of 2020 IEEE International Conference on Systems, Man, and Cybernetics*. IEEE, 2020, pp. 1081–1086.
- [76] L. Yang, X. Hu, and K. Li, “A vector angles-based many-objective particle swarm optimization algorithm using archive,” *Appl. Soft Comput.*, vol. 106, p. 107299, 2021.
- [77] J. Billingsley, W. Miao, K. Li, G. Min, and N. Georgalas, “Performance analysis of SDN and NFV enabled mobile cloud computing,” in *GLOBECOM’20: Proc. of 2020 IEEE Global Communications Conference*. IEEE, 2020, pp. 1–6.
- [78] J. Billingsley, K. Li, W. Miao, G. Min, and N. Georgalas, “Routing-led placement of vnfs in arbitrary networks,” in *CEC’20: Proc. of 2020 IEEE Congress on Evolutionary Computation*. IEEE, 2020, pp. 1–8.

- [79] S. Yuce and K. Li, “An enhancement of the NSGA-II reliability optimization using extended kalman filter based initialization,” in *UKCI’21: Proc. of the 20th UK Workshop on Computational Intelligence*, ser. Advances in Intelligent Systems and Computing, vol. 1409. Springer, 2021, pp. 121–128.
- [80] K. Li, K. Deb, and X. Yao, “R-metric: Evaluating the performance of preference-based evolutionary multiobjective optimization using reference points,” *IEEE Trans. Evolutionary Computation*, vol. 22, no. 6, pp. 821–835, 2018.
- [81] J. Cao, S. Kwong, R. Wang, X. Li, K. Li, and X. Kong, “Class-specific soft voting based multiple extreme learning machines ensemble,” *Neurocomputing*, vol. 149, pp. 275–284, 2015.
- [82] K. Li, R. Wang, S. Kwong, and J. Cao, “Evolving extreme learning machine paradigm with adaptive operator selection and parameter control,” *International Journal of Uncertainty, Fuzziness and Knowledge-Based Systems*, vol. 21, pp. 143–154, 2013.
- [83] K. Li, S. Kwong, R. Wang, J. Cao, and I. J. Rudas, “Multi-objective differential evolution with self-navigation,” in *SMC’12: Proc. of the 2012 IEEE International Conference on Systems, Man, and Cybernetics*, 2012, pp. 508–513.
- [84] K. Li, S. Kwong, and K. Deb, “A dual-population paradigm for evolutionary multiobjective optimization,” *Inf. Sci.*, vol. 309, pp. 50–72, 2015.
- [85] K. Li, K. Deb, Q. Zhang, and Q. Zhang, “Efficient nondomination level update method for steady-state evolutionary multiobjective optimization,” *IEEE Trans. Cybernetics*, vol. 47, no. 9, pp. 2838–2849, 2017.
- [86] J. Cao, S. Kwong, R. Wang, and K. Li, “AN indicator-based selection multi-objective evolutionary algorithm with preference for multi-class ensemble,” in *ICMLC’14: Proc. of the 2014 International Conference on Machine Learning and Cybernetics*, 2014, pp. 147–152.
- [87] —, “A weighted voting method using minimum square error based on extreme learning machine,” in *ICMLC’12: Proc. of the 2012 International Conference on Machine Learning and Cybernetics*, 2012, pp. 411–414.
- [88] K. Li, S. Kwong, R. Wang, K. Tang, and K. Man, “Learning paradigm based on jumping genes: A general framework for enhancing exploration in evolutionary multiobjective optimization,” *Inf. Sci.*, vol. 226, pp. 1–22, 2013.
- [89] K. Li, Á. Fialho, and S. Kwong, “Multi-objective differential evolution with adaptive control of parameters and operators,” in *LION5: Proc. of the 5th International Conference on Learning and Intelligent Optimization*, 2011, pp. 473–487.
- [90] K. Li and S. Kwong, “A general framework for evolutionary multiobjective optimization via manifold learning,” *Neurocomputing*, vol. 146, pp. 65–74, 2014.
- [91] K. Li, “Progressive preference learning: Proof-of-principle results in MOEA/D,” in *EMO’19: Proc. of the 10th International Conference Evolutionary Multi-Criterion Optimization*, 2019, pp. 631–643.
- [92] K. Li, J. Zheng, M. Li, C. Zhou, and H. Lv, “A novel algorithm for non-dominated hypervolume-based multiobjective optimization,” in *SMC’09: Proc. of 2009 the IEEE International Conference on Systems, Man and Cybernetics*, 2009, pp. 5220–5226.
- [93] J. Billingsley, K. Li, W. Miao, G. Min, and N. Georgalas, “A formal model for multi-objective optimisation of network function virtualisation placement,” in *EMO’19: Proc. of the 10th International Conference Evolutionary Multi-Criterion Optimization*, 2019, pp. 529–540.

- [94] K. Li, J. Zheng, C. Zhou, and H. Lv, “An improved differential evolution for multi-objective optimization,” in *CSIE’09: Proc. of 2009 WRI World Congress on Computer Science and Information Engineering*, 2009, pp. 825–830.
- [95] J. Zou, C. Ji, S. Yang, Y. Zhang, J. Zheng, and K. Li, “A knee-point-based evolutionary algorithm using weighted subpopulation for many-objective optimization,” *Swarm and Evolutionary Computation*, vol. 47, pp. 33–43, 2019.
- [96] K. Li, H. Nie, H. Gao, and X. Yao, “Posterior decision-making based on decomposition-driven knee point identification,” *IEEE Trans. Evol. Comput.*, 2021, accepted for publication.
- [97] J. Xu, K. Li, and M. Abusara, “Preference based multi-objective reinforcement learning for multi-microgrid system optimization problem in smart grid,” *Memetic Comput.*, vol. 14, no. 2, pp. 225–235, 2022.
- [98] G. Pruvost, B. Derbel, A. Liefoghe, K. Li, and Q. Zhang, “On the combined impact of population size and sub-problem selection in MOEA/D,” in *EvoCOP’20: Proc. of the 20th European Conference on Evolutionary Computation in Combinatorial Optimization*, ser. Lecture Notes in Computer Science, vol. 12102. Springer, 2020, pp. 131–147.
- [99] J. Wu, C. Luo, Y. Luo, and K. Li, “Distributed UAV swarm formation and collision avoidance strategies over fixed and switching topologies,” *IEEE Trans. Cybern.*, vol. 52, no. 10, pp. 10 969–10 979, 2022.
- [100] M. Wu, K. Li, S. Kwong, and Q. Zhang, “Evolutionary many-objective optimization based on adversarial decomposition,” *IEEE Trans. Cybern.*, vol. 50, no. 2, pp. 753–764, 2020.
- [101] K. Li, M. Liao, K. Deb, G. Min, and X. Yao, “Does preference always help? A holistic study on preference-based evolutionary multiobjective optimization using reference points,” *IEEE Trans. Evol. Comput.*, vol. 24, no. 6, pp. 1078–1096, 2020.
- [102] K. Li, R. Chen, D. A. Savic, and X. Yao, “Interactive decomposition multiobjective optimization via progressively learned value functions,” *IEEE Trans. Fuzzy Syst.*, vol. 27, no. 5, pp. 849–860, 2019.
- [103] M. Wu, S. Kwong, Y. Jia, K. Li, and Q. Zhang, “Adaptive weights generation for decomposition-based multi-objective optimization using gaussian process regression,” in *GECCO’17: Proc. of the 2017 Genetic and Evolutionary Computation Conference*. ACM, 2017, pp. 641–648.
- [104] L. Li, Q. Lin, K. Li, and Z. Ming, “Vertical distance-based clonal selection mechanism for the multiobjective immune algorithm,” *Swarm Evol. Comput.*, vol. 63, p. 100886, 2021.
- [105] G. Lai, M. Liao, and K. Li, “Empirical studies on the role of the decision maker in interactive evolutionary multi-objective optimization,” in *CEC’21: Proc. of the 2021 IEEE Congress on Evolutionary Computation*. IEEE, 2021, pp. 185–192.
- [106] X. Shan and K. Li, “An improved two-archive evolutionary algorithm for constrained multi-objective optimization,” in *EMO’21: Proc. of the 11th International Conference on Evolutionary Multicriteria Optimization*, ser. Lecture Notes in Computer Science, vol. 12654. Springer, 2021, pp. 235–247.
- [107] R. Wang, S. Ye, K. Li, and S. Kwong, “Bayesian network based label correlation analysis for multi-label classifier chain,” *Inf. Sci.*, vol. 554, pp. 256–275, 2021.
- [108] K. Li, Z. Xiang, T. Chen, and K. C. Tan, “BiLO-CPDP: Bi-level programming for automated model discovery in cross-project defect prediction,” in *ASE’20: Proc. of the 35th IEEE/ACM International Conference on Automated Software Engineering*. IEEE, 2020, pp. 573–584.

- [109] M. Liu, K. Li, and T. Chen, “DeepSQLi: deep semantic learning for testing SQL injection,” in *ISSTA’20: Proc. of the 29th ACM SIGSOFT International Symposium on Software Testing and Analysis*. ACM, 2020, pp. 286–297.
- [110] K. Li, Z. Xiang, T. Chen, S. Wang, and K. C. Tan, “Understanding the automated parameter optimization on transfer learning for cross-project defect prediction: an empirical study,” in *ICSE’20: Proc. of the 42nd International Conference on Software Engineering*. ACM, 2020, pp. 566–577.
- [111] J. Cao, H. Wang, S. Kwong, and K. Li, “Combining interpretable fuzzy rule-based classifiers via multi-objective hierarchical evolutionary algorithm,” in *SMC’11: Proc. of the 2011 IEEE International Conference on Systems, Man and Cybernetics*. IEEE, 2011, pp. 1771–1776.
- [112] S. Kumar, R. Bahsoon, T. Chen, K. Li, and R. Buyya, “Multi-tenant cloud service composition using evolutionary optimization,” in *ICPADS’18: Proc. of the 24th IEEE International Conference on Parallel and Distributed Systems*, 2018, pp. 972–979.
- [113] K. Li and Q. Zhang, “Decomposition multi-objective optimisation: current developments and future opportunities,” in *GECCO’19: Proc. of the 2019 Genetic and Evolutionary Computation Conference Companion*, 2019, pp. 1002–1031.
- [114] M. Liu, K. Li, and T. Chen, “Security testing of web applications: a search-based approach for detecting SQL injection vulnerabilities,” in *GECCO’19: Proc. of the 2019 Genetic and Evolutionary Computation Conference Companion*, 2019, pp. 417–418.
- [115] H. Gao, H. Nie, and K. Li, “Visualisation of pareto front approximation: A short survey and empirical comparisons,” in *CEC’19: Proc. of the 2019 IEEE Congress on Evolutionary Computation*, 2019, pp. 1750–1757.
- [116] K. Li, Z. Xiang, and K. C. Tan, “Which surrogate works for empirical performance modelling? A case study with differential evolution,” in *CEC’19: Proc. of the 2019 IEEE Congress on Evolutionary Computation*, 2019, pp. 1988–1995.
- [117] K. Li, K. Deb, and Q. Zhang, “Evolutionary multiobjective optimization with hybrid selection principles,” in *CEC’15: Proc. of the 2015 IEEE Congress on Evolutionary Computation*, 2015, pp. 900–907.
- [118] K. Li, K. Deb, O. T. Altinöz, and X. Yao, “Empirical investigations of reference point based methods when facing a massively large number of objectives: First results,” in *EMO’17: Proc. of the 9th International Conference Evolutionary Multi-Criterion Optimization*, 2017, pp. 390–405.
- [119] M. Wu, S. Kwong, Q. Zhang, K. Li, R. Wang, and B. Liu, “Two-level stable matching-based selection in MOEA/D,” in *SMC’15: Proc. of the 2015 IEEE International Conference on Systems, Man, and Cybernetics*, 2015, pp. 1720–1725.
- [120] X. Ruan, K. Li, B. Derbel, and A. Liefooghe, “Surrogate assisted evolutionary algorithm for medium scale multi-objective optimisation problems,” in *GECCO’20: Proc. of 2020 Genetic and Evolutionary Computation Conference*. ACM, 2020, pp. 560–568.
- [121] J. Xu, K. Li, and M. Abusara, “Multi-objective reinforcement learning based multi-microgrid system optimisation problem,” in *EMO’21: Proc. of the 11th International Conference on Evolutionary Multi-Criterion Optimization*, ser. Lecture Notes in Computer Science, vol. 12654. Springer, 2021, pp. 684–696.
- [122] R. Chen and K. Li, “Knee point identification based on the geometric characteristic,” in *SMC’21: Proc. of 2021 IEEE International Conference on Systems, Man, and Cybernetics*. IEEE, 2021, pp. 764–769.

- [123] P. N. Williams, K. Li, and G. Min, “Large-scale evolutionary optimization via multi-task random grouping,” in *SMC’21: Proc. of 2021 IEEE International Conference on Systems, Man, and Cybernetics*. IEEE, 2021, pp. 778–783.
- [124] H. Larochelle, D. Erhan, A. C. Courville, J. Bergstra, and Y. Bengio, “An empirical evaluation of deep architectures on problems with many factors of variation,” in *ICML’07: Proc. of the Twenty-Fourth International Conference on Machine Learning*, ser. ACM International Conference Proceeding Series, vol. 227. ACM, 2007, pp. 473–480.
- [125] P. N. Williams, K. Li, and G. Min, “Black-box adversarial attack via overlapped shapes,” in *GECCO ’22: Genetic and Evolutionary Computation Conference, Companion Volume, Boston, Massachusetts, USA, July 9 - 13, 2022*. ACM, 2022, pp. 467–468.
- [126] S. Zhou, K. Li, and G. Min, “Attention-based genetic algorithm for adversarial attack in natural language processing,” in *PPSN’22: Proc. of 17th International Conference on Parallel Problem Solving from Nature*, ser. Lecture Notes in Computer Science, vol. 13398. Springer, 2022, pp. 341–355.
- [127] S. Li, K. Li, and W. Li, “Do we really need to use constraint violation in constrained evolutionary multi-objective optimization?” in *PPSN’22: Proc. of the 17th International Conference on Parallel Problem Solving from Nature*, ser. Lecture Notes in Computer Science, vol. 13399. Springer, 2022, pp. 124–137.
- [128] S. Zhou, K. Li, and G. Min, “Adversarial example generation via genetic algorithm: a preliminary result,” in *GECCO’22: Proc. of the 2020 Genetic and Evolutionary Computation Conference*. ACM, 2022, pp. 469–470.
- [129] Q. Yang, Y. Zhang, W. Dai, and S. J. Pan, *Transfer Learning*. Cambridge University Press, 2020.
- [130] T. M. Hospedales, A. Antoniou, P. Micaelli, and A. J. Storkey, “Meta-learning in neural networks: A survey,” *IEEE Trans. Pattern Anal. Mach. Intell.*, vol. 44, no. 9, pp. 5149–5169, 2022.
- [131] K. C. Tan, L. Feng, and M. Jiang, “Evolutionary transfer optimization - A new frontier in evolutionary computation research,” *IEEE Comput. Intell. Mag.*, vol. 16, no. 1, pp. 22–33, 2021.
- [132] L. Chen, H. Liu, K. C. Tan, and K. Li, “Transfer learning-based parallel evolutionary algorithm framework for bilevel optimization,” *IEEE Trans. Evol. Comput.*, vol. 26, no. 1, pp. 115–129, 2022.